ANL-HEP-TR-96-27

HIGH ENERGY PHYSICS DIVISION SEMIANNUAL REPORT OF RESEARCH ACTIVITIES

January 1, 1995 - June 30, 1995

ARGONNE NATIONAL LABORATORY

Argonne, Illinois

Operated by THE UNIVERSITY OF CHICAGO for the

U.S. DEPARTMENT OF ENERGY

under Contract W-31-109-Eng-38

ANL-HEP-TR-96-27

Argonne National Laboratory
9700 South Cass Avenue
Argonne, Illinois 60439

HIGH ENERGY PHYSICS DIVISION SEMIANNUAL REPORT OF RESEARCH ACTIVITIES

January 1, 1995 - June 30, 1995

Prepared from information gathered and edited by
the Committee for Publications and Information:

Members:
R. Wagner
P. Schoessow
R. Talaga

December 1995

Contents

I Experimental Research Program 2

I.A Experiments with Data . . . 2

I.A.1 Medium Energy Polarization Program . . . 2

I.A.2 Polarized Proton Physics at Fermilab . . . 2

I.A.3 Collider Detector at Fermilab . . . 7

I.A.4 Non-Accelerator Physics at Soudan . . . 16

I.A.5 ZEUS Detector at HERA . . . 22

I.B Experiments in Planning or Construction Phase . . . 34

I.B.1 STAR Detector for RHIC . . . 34

I.B.2 Main Injector Neutrino Oscillation Search . . . 36

I.B.3 ATLAS Detector Research & Development . . . 39

I.C Detector Development . . . 42

I.C.1 ATLAS Hadron Calorimeter and Trigger Development . . . 42

II Theoretical Physics Program 50

II.A Theory . . . 50

II.A.1 Precise Calculation of the Cross Section for Top Quark Production . . . 50

II.A.2 Prompt Photon plus Associated Heavy Flavor at Next-to-Leading Order in QCD . . . 50

II.A.3 Canonical Dual Transformations and Supersymmetry . . . 51

II.A.4 Higher-order BFKL Evolution . . . 52

II.A.5 Gauge Theory High-Energy Behavior from j-plane Unitarity . . . 52

II.A.6 Lattice Measurement of Matrix Elements for Decays of Heavy Quarkonium . 52

II.A.7 Inclusive Prompt Photon Production in Photon-Photon Collisions . . . 53

II.A.8 Analysis of Recent Polarization Experiments . . . 53

II.B Computational Physics . . . 54

III Accelerator Research & Development Program 56

III.A High Resolution Profile Monitor Development . . . 56

IV Publications 57

V Colloquia and Conference Talks 63

VI High Energy Physics Community Activities 64

VII High Energy Physics Division Reasearch Personnel 66

Abstract

This report describes the research conducted in the High Energy Physics Division of Argonne National Laboratory during the period of January 1, 1995 - July 31, 1995. Topics covered here include experimental and theoretical particle physics, advanced accelerator physics, detector development, and experimental facilities research. Lists of division publications and colloquia are included.

I EXPERIMENTAL RESEARCH PROGRAM

I.A EXPERIMENTS WITH DATA

I.A.1 Medium Energy Polarization Program

Spin effects in proton-proton (*pp*) and neutron-proton (*np*) scattering have been studied for many years in the medium energy polarization program. Data from these experiments have been combined with other measurements in order to determine nucleon-nucleon amplitudes, which are needed to understand the strong interaction at intermediate energies and nucleon scattering from nuclei. They will become more important in the future to interpret a variety of electron scattering experiments at CEBAF. These spin data are also important to investigate energy-dependent structure seen in various nucleon-nucleon spin observables and other reactions.

A major paper describing final results for four *np* elastic scattering spin observables (C_{SS}, $C_{SL} = C_{LS}$, C_{LL}, C_{NN} - see Figures 1-4) with a polarized neutron beam incident on a polarized proton target is nearly complete and should be submitted for publication in the next several months. The data from these LAMPF experiments are shown in the figures as solid circles, and results from other groups as open circles, squares, and triangles. The curves are from phase shift predictions of Arndt *et al.* (solid) and Bugg (dashed), and from a model prediction by Lee *et al.* (dot-dashed); many of the present data were included in the phase shift data bases. Generally good agreement is seen with other experiments and the predictions. These results have had a major impact on the isospin-0 nucleon-nucleon amplitude determinations from 500 to 800 MeV, which are becoming well known for the first time.

Work has begun again on a partially written paper describing LAMPF measurements of $n+p \rightarrow d+\pi$ spin observables. The analysis is being completed at the University of Montana and some of the writing is occurring at Washington State University. Additional paper writing, physics interpretation, and preparation of figures is taking place at ANL. It is hoped to produce a complete draft of the major paper by late fall.

Measurements of *pp* elastic scattering were performed at Saclay in April. Data were collected at 800 MeV to check the absolute target polarization, 2040 and 2230 MeV to calibrate older data collected, and 2350, 2450, 2520, 2580, and 2800 MeV to search for higher energy structure in the spin observables $P = A_{oono}$, C_{NN}, D_{NN}, and K_{NN}. These data will also be very useful in the future to measure beam polarizations at new accelerators, such as LISS. Modifications to the data analysis program are being implemented to better monitor variations in chamber and scintillation counter efficiencies. Such changes can lead to serious systematic errors in the results. Also, all scaler data from runs in April, 1995, May/June, 1994, and November/December, 1993 were read and checked from the magnetic tapes. This analysis will all be done at ANL as part of a Ph.D. thesis for C. Allgower.

(H. Spinka)

I.A.2 Polarized Proton Physics at Fermilab

i) We have completed a paper on "Analyzing Power Measurement in Inclusive Lambda Production with a 200-GeV/c Polarized Proton Beam" and sent it to *Phys. Rev. Lett.* for publication. The

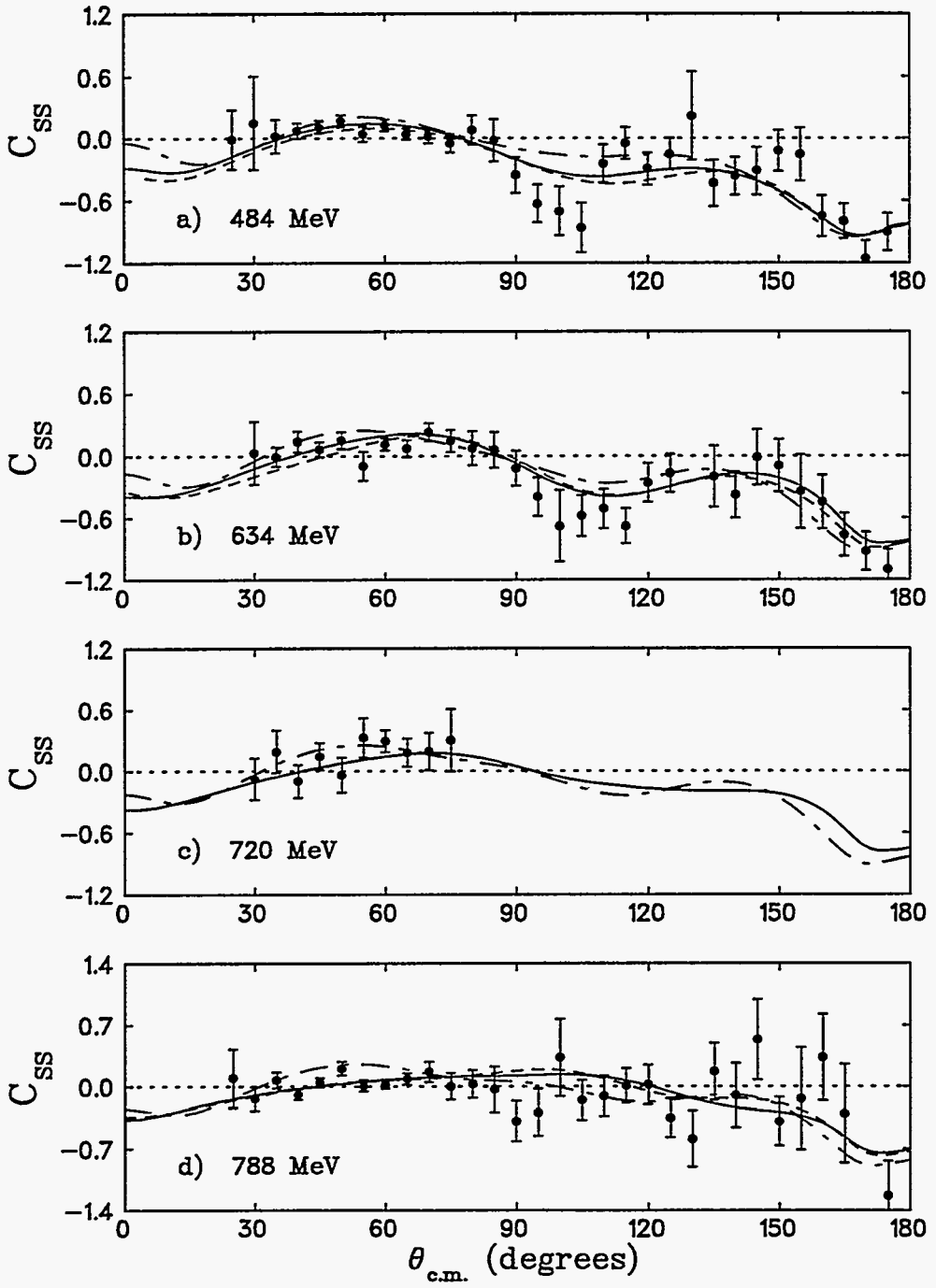

Figure 1: Measurements of the *np* elastic scattering spin parameter C_{SS} from LAMPF. The solid and dashed lines are from the phase shift solutions of R.A. Arndt *et al.* and D.V. Bugg, and the dot-dashed line from a model prediction of T.S.H. Lee *et al.* .

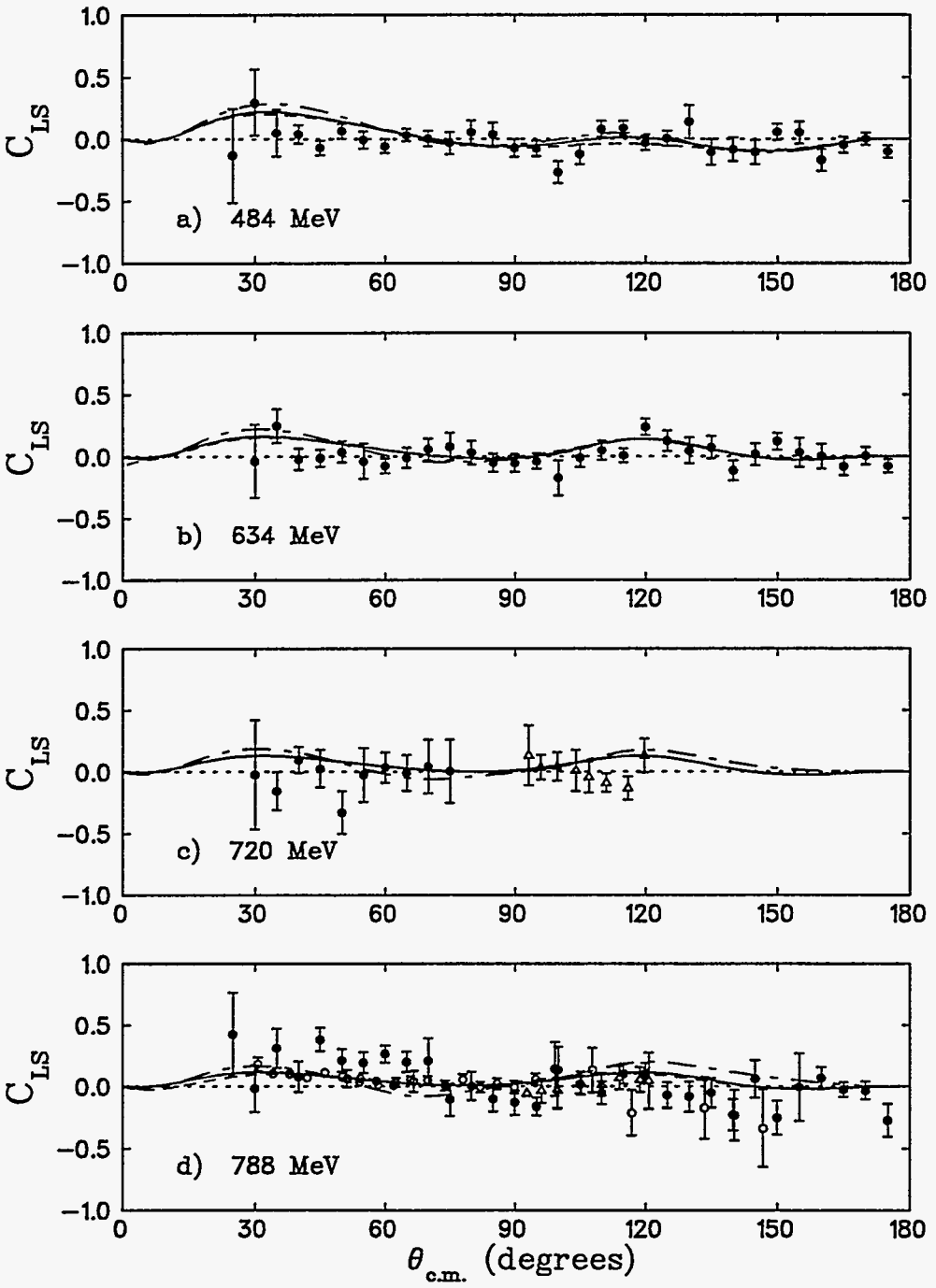

Figure 2: Measurements of the *np* elastic scattering spin parameter C_{LL} from LAMPF. The solid and dashed lines are from the phase shift solutions of R.A. Arndt *et al.* and D.V. Bugg, and the dot-dashed line from a model prediction of T.S.H. Lee *et al.* .

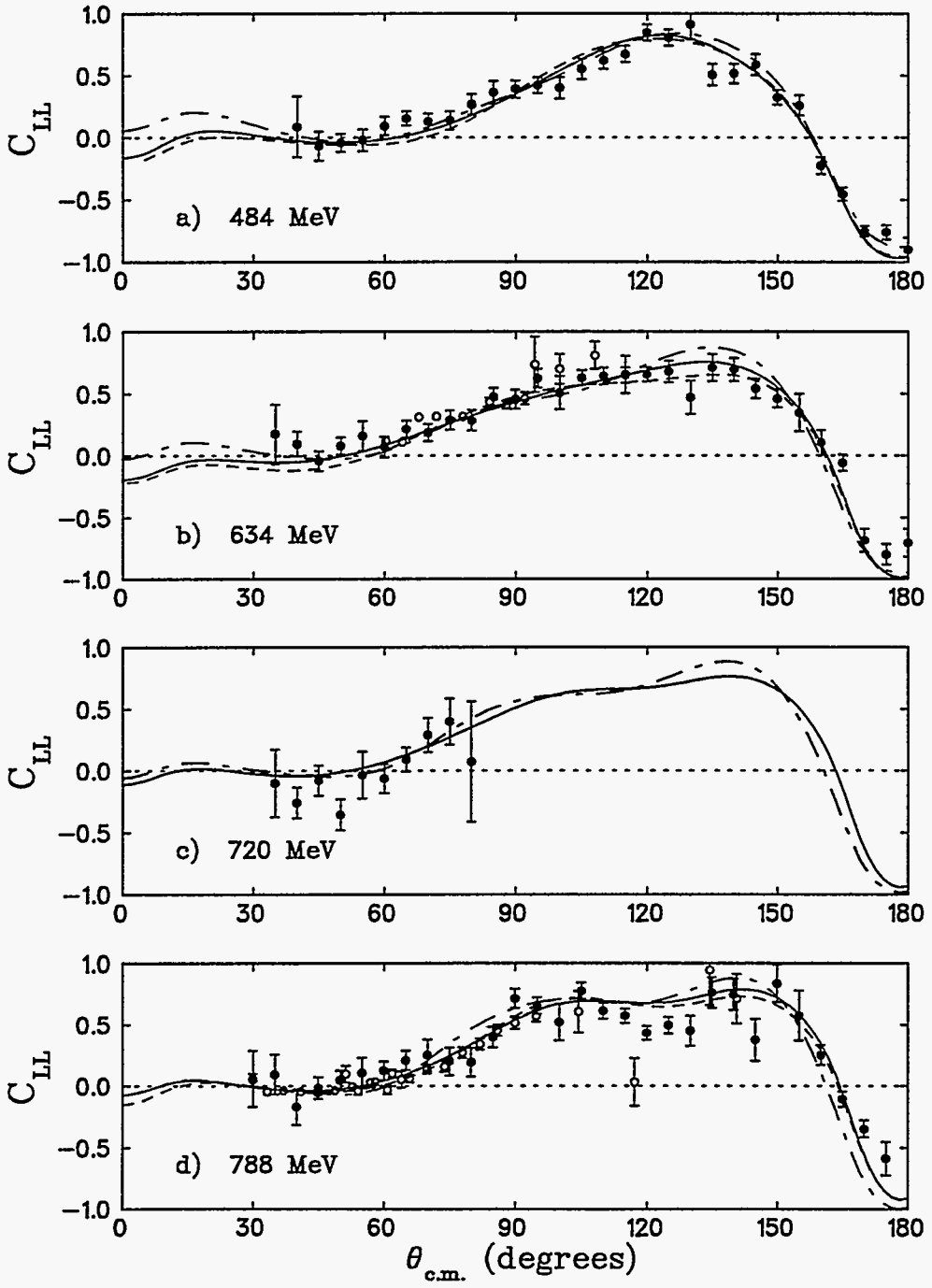

Figure 3: Measurements of the *np* elastic scattering spin parameter C_{LS} from LAMPF. The solid and dashed lines are from the phase shift solutions of R.A. Arndt *et al.* and D.V. Bugg, and the dot-dashed line from a model prediction of T.S.H. Lee *et al.* .

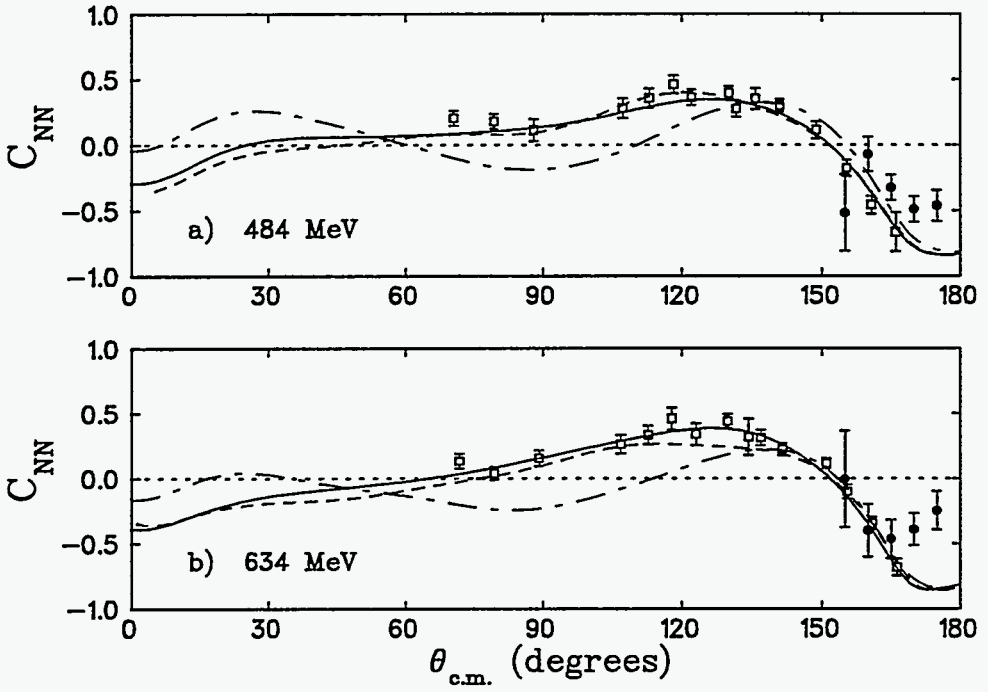

Figure 4: Measurements of the *np* elastic scattering spin parameter C_{NN} from LAMPF. The solid and dashed lines are from the phase shift solutions of R.A. Arndt *et al.* and D.V. Bugg, and the dot-dashed line from a model prediction of T.S.H. Lee *et al.* .

covered kinematic range is $0.2 \leq x_F \leq 1.0$ and $0.1 \leq p_T \leq 1.5$ GeV/c. The data indicate a negative asymmetry at large x_F and moderate p_T . These results can further test the current ideas on the underlying mechanisms for the well known considerable polarization of hyperons.

ii) We have completed a paper on "Single-Spin Asymmetries and Invariant Cross Sections of the High Transverse-Momentum Inclusive π^0 Production in 200-GeV/c pp and $\overline{p}p$ Interactions" and sent it to *Phys. Rev.* for publication. The measured asymmetries are consistent with a value of zero, within the error bars for p_T up to 4.5 GeV/c, and are consistent with perturbative QCD expectations.

iii) We are completing a paper on "The Difference Between the pp and $\overline{p}p$ Total Cross Sections with Spins Antiparallel and with Spins Parallel Longitudinally at 200 GeV/c".

iv) The following reactions will be investigated:

- $\eta(550), \omega(783)$,and K^0_S (500) production in pp and $\overline{p}p$ at large x_F.
- A_{LL} in π° production in pp and $\overline{p}p$ with associated charged particles.
- Asymmetry in Drell-Yan production.

(A. Yokosawa)

I.A.3 Collider Detector at Fermilab

a. Physics Results

i. Top Quark Observed

Using the 20 pb^{-1} integrated luminosity 1992-1993 data set, we previously announced evidence for production of top quark pairs. Using an additional 47 pb^{-1} from the ongoing run, the statistical significance of the signal became undeniable. Further developments in the top analysis included development of new vertex tag code, dissipation of the apparent excess of tagged Z events and the apparent shortage on background $W + 4$ jet events, and the reduction of the measured cross section by a combination of better understood tagging efficiency and better statistics. After the required notification of D0, a letter, without any hedges about not firmly established, was submitted. The D0 collaboration went concurred in the observation.

The direct measurement of the top mass has a profound effect on the global electroweak precision measurement fits. Our value, $m_{top} = 176 \pm 8(\text{stat}) \pm 12(\text{sys})$ GeV/c^2 is in agreement with indirect inference from the fits and is already more precise. The tagged fit mass peak is shown in Figure 5. The systematic uncertainty is dominated by final state gluon effects; data constraints on such effects should allow better measurement in the future. Steve Kuhlmann helped organize a CTEQ workshop on such things. Marcus Hohlmann is studying the presence and effect of τs in the top signal.

ii. W Mass Measurement

Various groundwork for the run 1b measurement is going on. A Purdue student, Adam Hardman will be joining us for this effort in the fall. Barry Wicklund continued his study of photon

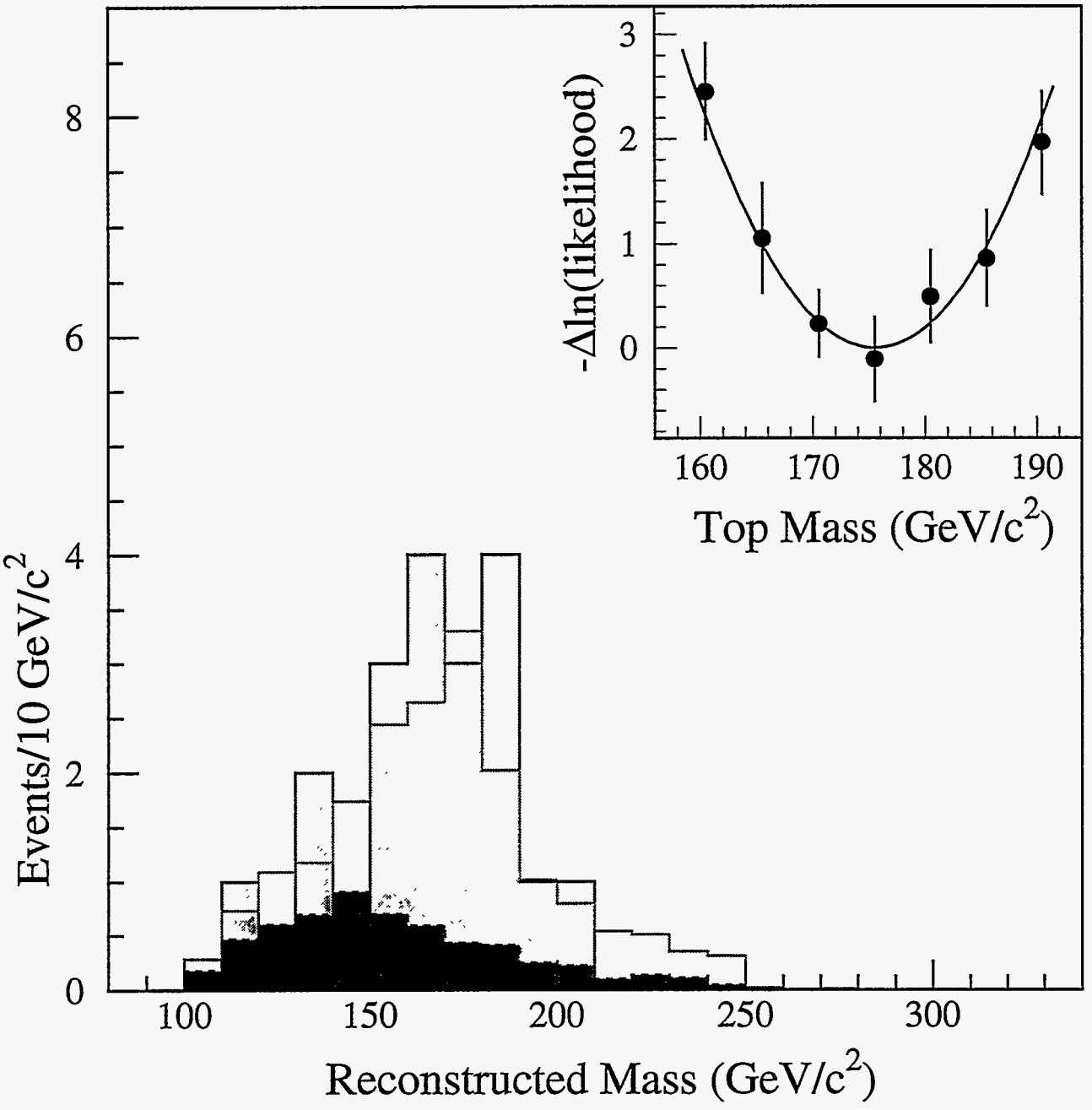

Figure 5: The fit mass distribution for tagged events from the observation PRL sample. The dark shaded area is the backgound, constrained in the fit to be consistent with counting expectations. The solid shaded histogram is the data.

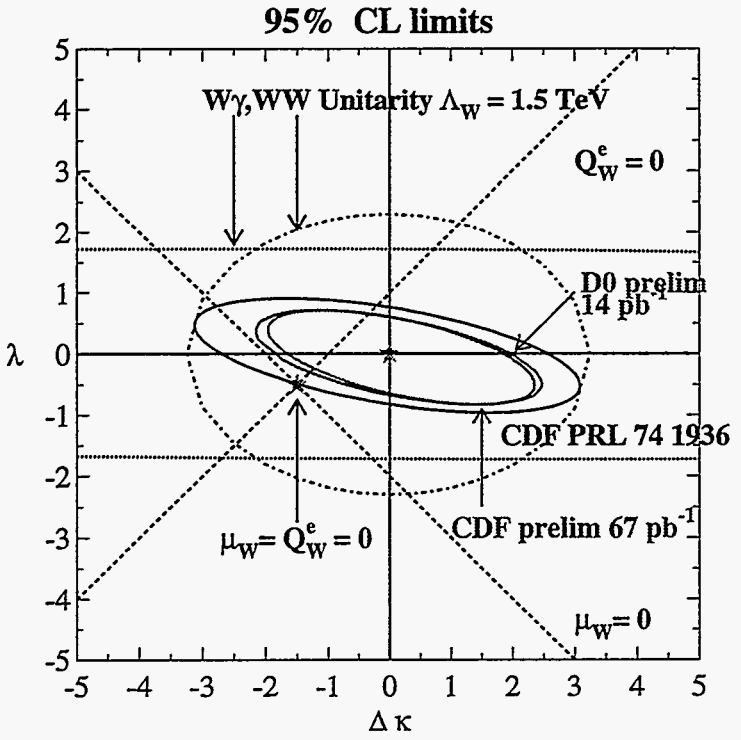

Figure 6: The limit contours for $W\gamma$ coupling.

conversions in run 1a showing in detail that the nominal CDF simulation is not so bad for material. We are developing a conversion based strategy for understanding material effects. Larry Nodulman provided a preliminary central EM calibaration for use in initial studies and other run 1b analyses such as the top mass.

iii. Vector Boson Couplings

Bob Wagner and Theresa Fuess continued their work on trilinear boson couplings. For the $\bar{p}p$ conference, the $W\gamma$ and $Z\gamma$ analyses were updated to use the total of 67 pb^{-1} from the whole of run 1. The limits on $\Delta\kappa$ and λ for anomalous W couplings are shown in Figure 6 and the limits for anomalous Z coulings in Figure 7. Acceptance is being extended to plug photons and perhaps electrons, and progress is being made toward demonstrating the guage interference radiation zero.

iv. High E_T Jets

The excess of jet production at high $E_{\rm T}$ has persisted in CDF data, as seen in Figure 8. Steve Kuhlmann is working with his CTEQ colleagues on an investigation of the possible contribution of parton distributions to the high $p_{\rm T}$ jet excess using the CTEQ QCD package at ANL. An increase in the high-x gluon distribution could, in principle, explain part of the excess. The evaluation of other data sets with these high-x gluons is under way.

v. Direct Photons

Steve Kuhlmann has continued his photon work studying the photon+jet angular distribu-

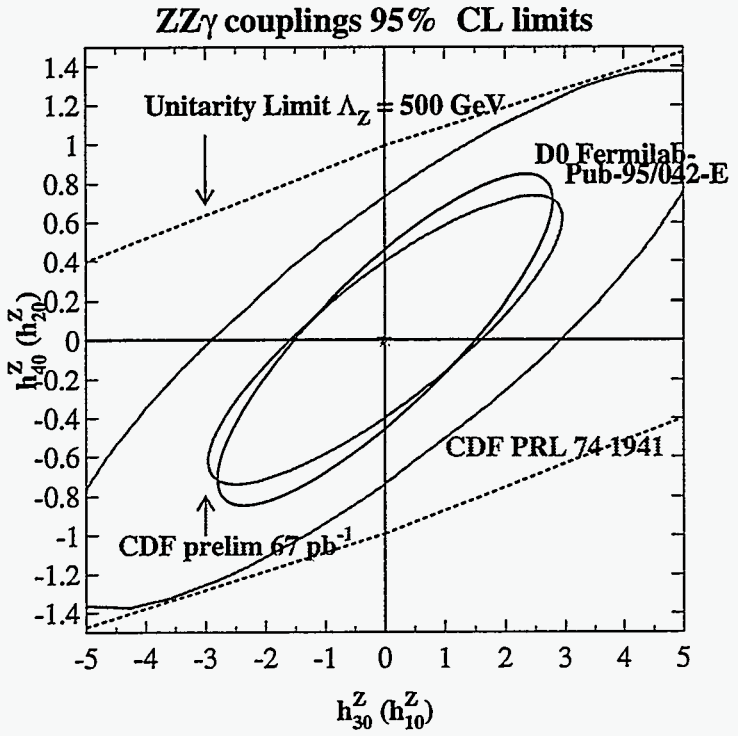

Figure 7: The limit contours for $Z\gamma$ coupling.

tion, seen in Figure 9, which has been measured to a precision greater than dijets and W production. Unlike the dijet and W data, which agree well with NLO QCD, the photon data is slightly steeper than QCD, which may be due to photon fragmentation processes.

vi. Diphoton Production

Bob Blair has continued his work on diphotons. Previously results for the diphoton spectrum for CDF run 1a data were reported only for the high E_T end of the diphoton spectrum. Figure 10 shows the cross section versus photon E_T (each event counts twice in this plot, once at the E_T of each of its two photons). The method used to extract the photon-photon contribution as distinct from the background contribution is essentially identical to the method described in F. Abe *et al.* , Phys. Rev. Lett. **70**, 2232 (1993). The photon candidate cuts include a transverse energy cut of $E_T > 10$ GeV. Both of the photon candidates must have less than 4 GeV in a cone of 0.7 (in $\eta - \phi$ space) around them and one of the candidates must have less than 2 GeV around it. To distinguish between background and photons for candidates with $E_T > 35$ GeV, the preshower pulse height is used instead of the lateral profile measured at shower maximum. The results for the 12.8 pb^{-1} 1992-1993 data set are compared to the data from the 1988-1989 run. Both data sets are reasonably consistent with the NLO QCD prediction.

One quantity of interest that can be measured using the low E_T diphoton sample is the distribution of the diphoton system p_T . This is a measure of how much the hard scatter, which produces the two photons, is boosted by initial and final state soft gluon emmision. Figure 11 shows the measured distribution along with the predictions of the NLO calculation and the PYTHIA Monte Carlo. The NLO QCD prediction clearly underestimates the effect of this smearing, while

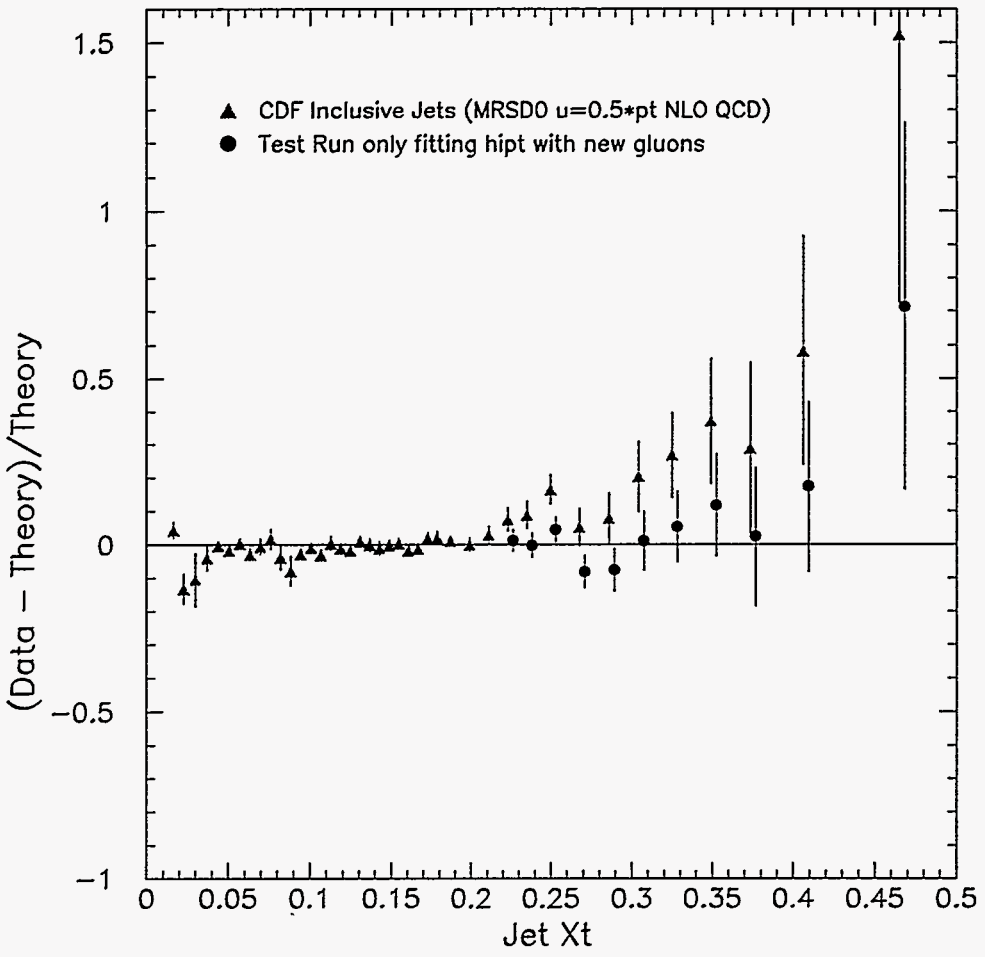

Figure 8: Jet E_T spectrum on a linear scale, normalized to QCD expectation, showing variability of the QCD prediction with different gluon structure.

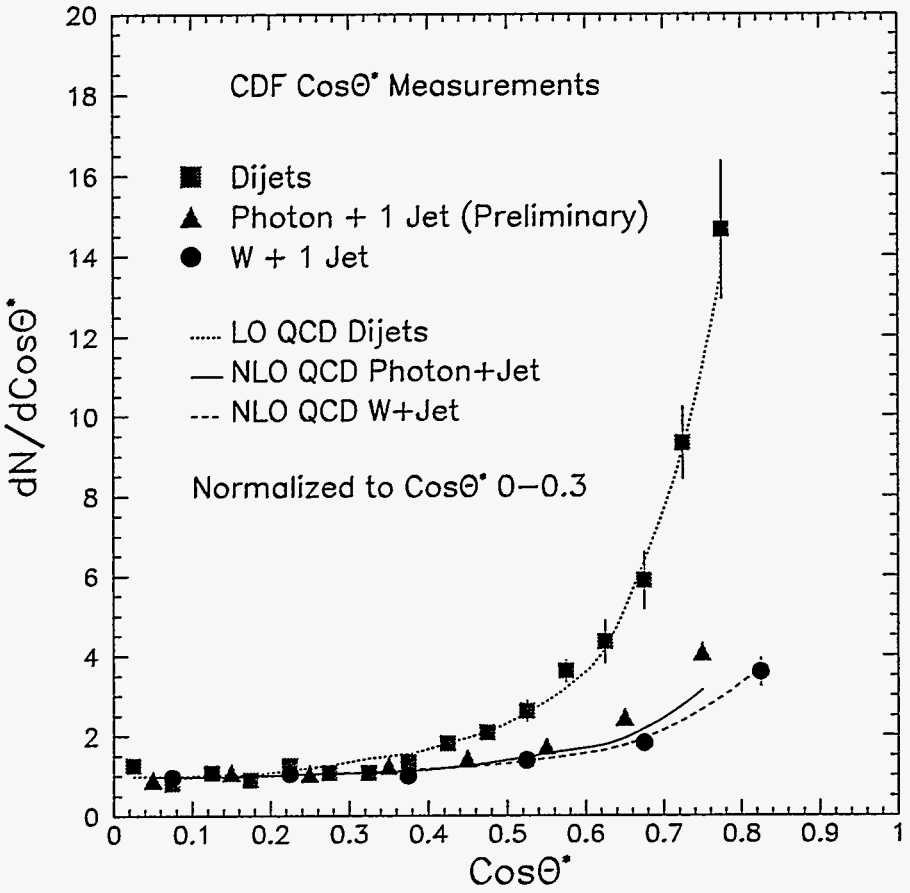

Figure 9: The $\cos\theta^*$ distribution comparing γ-jet, dijet and W-jet data to QCD predictions.

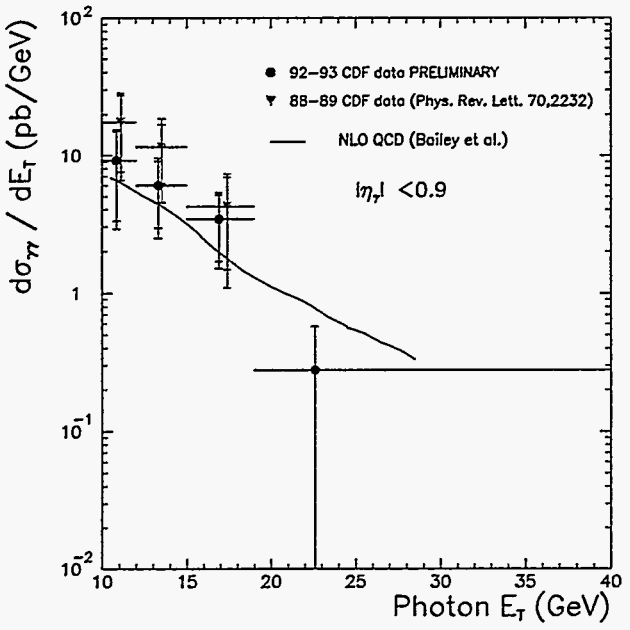

Figure 10: Photon E_T distribution for 88/89 data and 92/93 data for diphoton candidates.

PYTHIA appears to agree reasonably well.

vii. *b* Physics

Karen Byrum and Barry Wicklund are continuing their work on measuring the b cross section using inclusive electrons. Interest in this area has been peaked by the consistently 2-3 times higher than expected observed b cross sections and even higher prompt ψ and ψ' cross sections. Low energy running will help to check against UA1 cross sections which agreed with the predictions.

b. CDF Summary of Active Data Taking

The current round of data taking, run 1b, continued to a summer shutdown toward the end of July. An additional 50 pb^{-1} of data has been collected to tape this year, for a total sample for all run 1 of about 110 pb^{-1} . Peak luminosity has approached $3 \times 10^{31} cm^{-2} s^{-1}$. Most detectors have continued to perform well. Cooler operation and shorter gates have preserved the good signal to noise in the silicon vertex detector, and lowered high voltage has preserved the operability of the plug hadron calorimeter. A serious problem with the central tracking chamber (CTC) was discovered by Jimmy Proudfoot while investigating track trigger efficiency using notrack electron triggers (see Figure 12). While the track trigger efficiency is reduced as expected with instantaneous luminosity, it also falls with cumulative luminosity. This has been shown to be, in fact, wire aging in the CTC. While the track trigger efficiency has been largely restored by changes to the algorithm de-emphasizing inner layers, the aging, which is > 20 times faster than expected, has not been understood. Given that the design luminosity for CDF was 10 pb^{-1} from 10 years at $10^{30} cm^{-2} s^{-1}$, we are not doing too badly.

Offline reconstruction is keeping up fairly well and the central EM and associated detectors

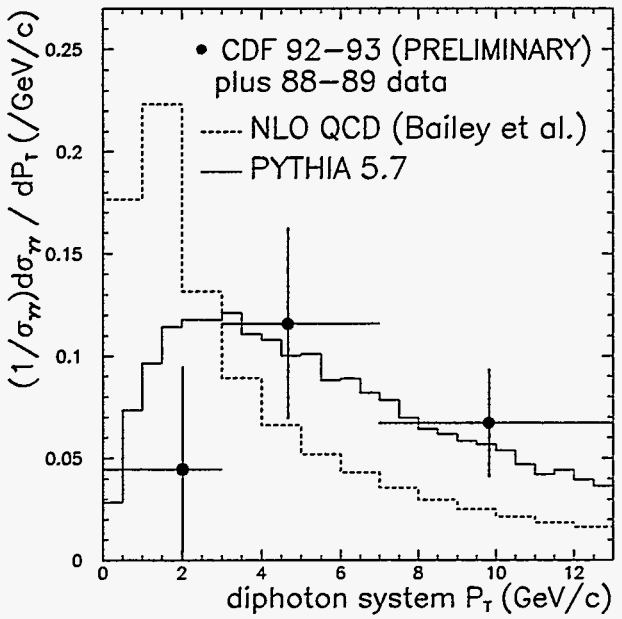

Figure 11: The distribution in diphoton system p_{T} using both data samples (1989-90 and 1992-93).

which are the rsponsibility of the Argonne group have behaved reasonably well.

Marcus Hohlmann and Larry Nodulman have continued supporting the monitoring of data quality. Bob Blair rotated out as a shift leader and Steve Kuhlmann and Larry Nodulman have begun cycles of being shift leaders.

c. CDF Planned Activities and Planning Issues

Running will resume in October and continue through at least February. The coming period should produce about 25 pb^{-1} of additional normal data as well as various special runs including 2 weeks at 630 GeV and a couple weeks at 2 TeV. Additional special running is planned for CDF diffraction studies using Roman pots to be installed along with microplug detectors. Various other sample test detectors are also being installed during the summer shutdown.

Larry Nodulman, Barry Wicklund, and others helped to produce summary documents for the detector upgrades and physics of run 2. The PAC and the laboratory have redefined run 2 to start at a luminosity of $10^{32} cm^{-2} s^{-1}$ and grow by a factor 2 or more from there. A permanent magnet antiproton recycler ring in the main injector tunnel is included. This implies that CDF will replace the CTC for run 2, and funding is allocated accordingly. The Argonne group, with Bob Wagner at the point, is becoming involved in replacing the CTC. Two alternatives are being considered: a smaller cell version like the CTC which would give optimum performance due to low mass and thus minimal multiple scattering for $1 - 2 \times 10^{32}\ cm^{-2} s^{-1}$; and a straw system which would have more material but would have performance which would be less degraded by even higher luminosity. We are currently working at Argonne on the mechanics of a straw design.

We have agreed on an MOU for front end work for run 2 but progress has been slow in

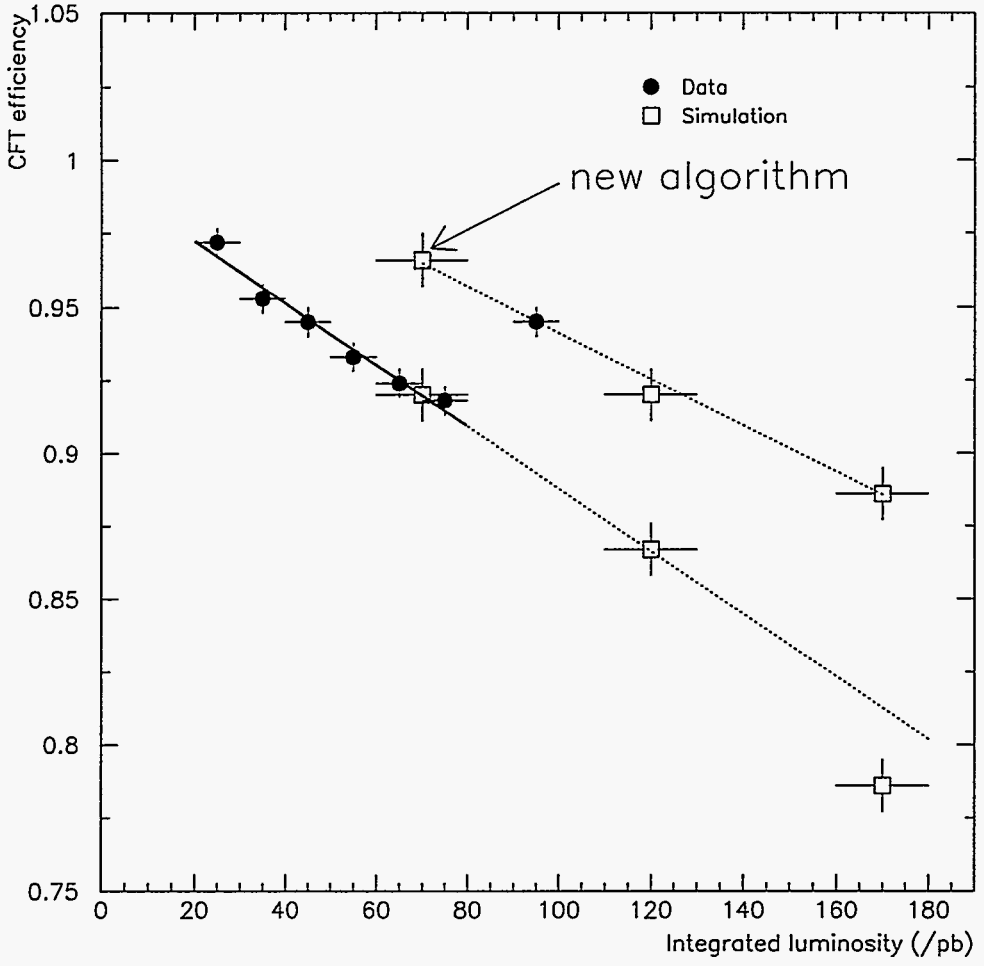

Figure 12: The efficiency of the CFT track trigger versus accumulated luminosity.

hardware as we continue to await a test stand to be set up at Argonne for working on preamplifiers feeding QIEs (current splitters for FADCs).

The current expectation for run 2 is to roll the detector in during the late spring of 1999 and to collect 2 fb^{-1} in the first 2 years. But as even John Peoples admitted at the Users Meeting, such schedules tend to lengthen by a factor 1.4. Fortunately this still leaves run 2 with plenty of opportunity for doing good physics in the pre-LHC era.

Development of options for even higher luminosity has been discussed by the TeV2000 group, with Steve Kuhlmann, Bob Wagner, Theresa Fuess and Larry Nodulman participating. This task is to be taken over by a Fermilab group in the computing division, like the dedicated b detector study, but with CDF and D0 participation. A TeV2000 report document is being prepared.

(L. Nodulman)

I.A.4 Non-Accelerator Physics at Soudan

a. Physics Results

In early 1995 Soudan physicists completed the upgrade of the Monte Carlo simulation software needed for the final analysis of Soudan 2 neutrino data. The initial goal of this analysis is to measure the ν_μ/ν_e ratio from atmospheric neutrino interactions in Soudan 2. Differences between measured ratios and those predicted by Monte Carlo simulations have been interpreted by other experiments as evidence for neutrino oscillations.

Approximately two fiducial kiloton years of atmospheric neutrino data have been recorded by Soudan 2 since operation began in 1988. The data sample has been divided into four half-kiloton year samples for analysis purposes. A preliminary analysis of the first two samples was completed in 1993, using an early version of the Monte Carlo simulation. The new simulation software provides a more accurate representation of neutrino interactions and of the detector response to particles produced in these interactions. The new Monte Carlo software is now being used in the analysis of the third half-kiloton year data sample. It will also be used for all subsequent data samples, and for the reanalysis of the first two half-kiloton year data samples.

A large sample of new Monte Carlo neutrino interaction events is being analyzed along with contained events from the third half kiloton year data set. Monte Carlo events are processed by the same software as Soudan 2 data events, and are mixed with data events for the final physicist scan of the contained event sample. The physicist classification of contained events is an inherently subjective process involving pattern recognition skills and physics judgements. In the new analysis procedure, the physicist scan is being carried out by two independent teams on a mixed, unlabeled sample of Monte Carlo and data events. Comparison of event classifications made by the two analysis teams will give a measure of the systematic uncertainty of the scanning process. Comparison of the classification of Monte Carlo events with the actual generated event types will measure the event classification confusion matrix. (The two scan teams met to compare their results for the third half-kiloton year sample in mid July.)

Soudan 2 data are also being used for a number of ongoing cosmic-ray physics analyses, which will be the subjects of several Ph.D. theses. These include the use of underground muon tracks to search for astrophysical point sources and for large-scale anisotropies of cosmic rays. The collaboration also continued the study of primary cosmic ray composition using multiple muon

events, with and without coincidence data from surface detectors which observe the parent air showers directly. The results of an initial coincidence experiment between Soudan 2 and a 40 m^2 surface array were submitted to *Physical Review D* in 1994 and have now been accepted for publication.

The study of multiple muon events in the Soudan 2 detector alone, without the use of surface array data, is the subject of the Ph.D. thesis of University of Minnesota student Sue Kasahara. Monte Carlo simulations of the cosmic ray air showers which produce multiple muon events in Soudan 2 show that the multiplicity distribution is sensitive to the nuclear composition of the cosmic ray primaries which initiate air showers. Figure 13 shows a computer reconstruction of a high multiplicity multiple muon event in Soudan 2. Figure 14 shows the energy dependent nuclear compositions of the three different models used in the analysis, and Figure 15 shows a preliminary comparison between the data and multiplicity distributions predicted by the three composition models. These preliminary Soudan 2 results favor a "light" nuclear composition of the cosmic ray primaries in the interesting "knee" region (~1000 TeV/nucleus). This model is compatible with an extra-galactic origin of cosmic ray primaries in the knee region, where Active Galactic Nuclei may be responsible for cosmic ray acceleration.

b. Experimental Apparatus Improvement

The upgrade of Soudan 2 calorimeter modules continued throughout the first half of 1995. Eight of the worst-performing modules were removed from the north half of the detector to improve wireplane gain uniformity and to repair leaks. A total of 17 modules which had previously been removed from the detector were repaired at Soudan during the first half of the year. In addition, all six of the modules which had been shipped to Argonne during 1994 were returned to Soudan during the winter and spring of 1995. Five of the six modules were completely rebuilt (only the corrugated steel sheets were saved) and a drift high voltage fault in the sixth module was repaired. Three detector halfwalls, which had been disassembled earlier, were brought back into operation during the six-month period. (A halfwall is a subassembly of eight 5-ton modules, stacked four across and two high.) In addition, anode high voltage splitter hardware was installed on nearly all remaining halfwalls, so that each individual wireplane may be operated at its own optimum high voltage. At the end of June, all but four halfwalls were back in operation, bringing the total operating mass to 826 tons.

Other installation activities included the deployment of 12 new active shield proportional tubes, covering small gaps between ceiling and wall panels. These gaps constituted only a few percent of the total solid angle coverage provided by the active shield, but required special short tubes which were quite labor intensive to build and install.

The south half of the new Oxford "crack filler" array was installed during the month of June. Data acquisition from this new detector is scheduled to begin later in the year. This array of proportional tubes is being installed immediately above the upper layer of Soudan 2 calorimeter modules. The array makes use of tubes built originally for the Tasso detector at DESY. It will provide enhanced protection from cosmic ray muons which might enter the calorimeter undetected through cracks between modules and halfwalls. Such protection is already provided by the cavern-liner active shield which has been in operation for many years. While the original shield is still thought to provide adequate coverage, crack-penetrating muons are potentially such a serious background for neutrino and nucleon decay events that the redundancy provided by the new crack filler array is very important, if only to confirm the effectiveness of the original shield. The installation of the North half of the crack-filler active shield array is planned for the latter half of 1995, following the completion of the calorimeter module upgrade project.

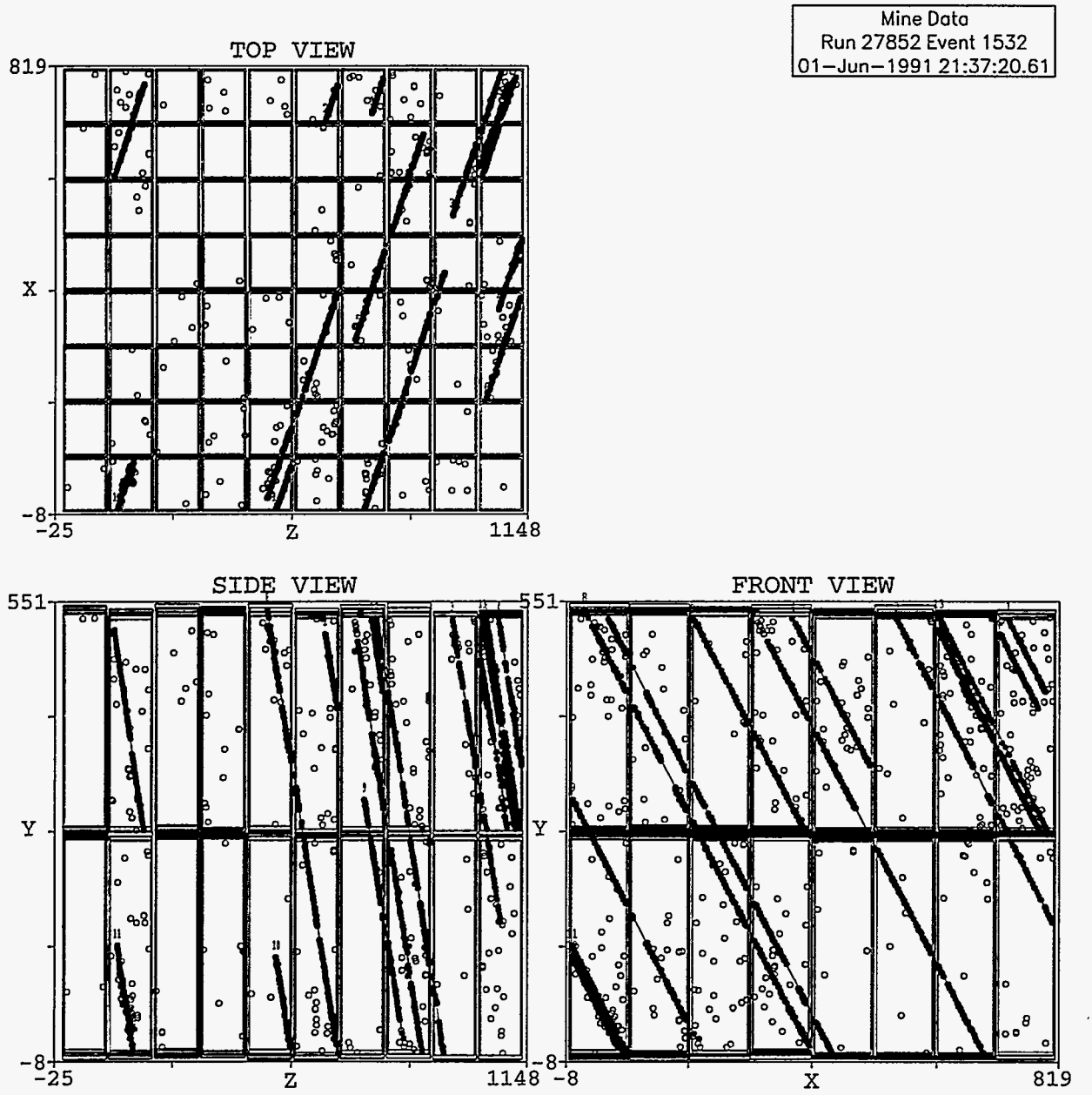

Figure 13: A 14 muon event in the Soudan 2 detector. The figure shows three orthogonal views of the same event. Distances are given in centimeters. Hits which are not associated with reconstructed tracks (superimposed straight lines) are the result of improperly demultiplexed data, and do not affect the total track count. All 14 parallel muons originated from a single cosmic ray shower in the upper atmosphere.

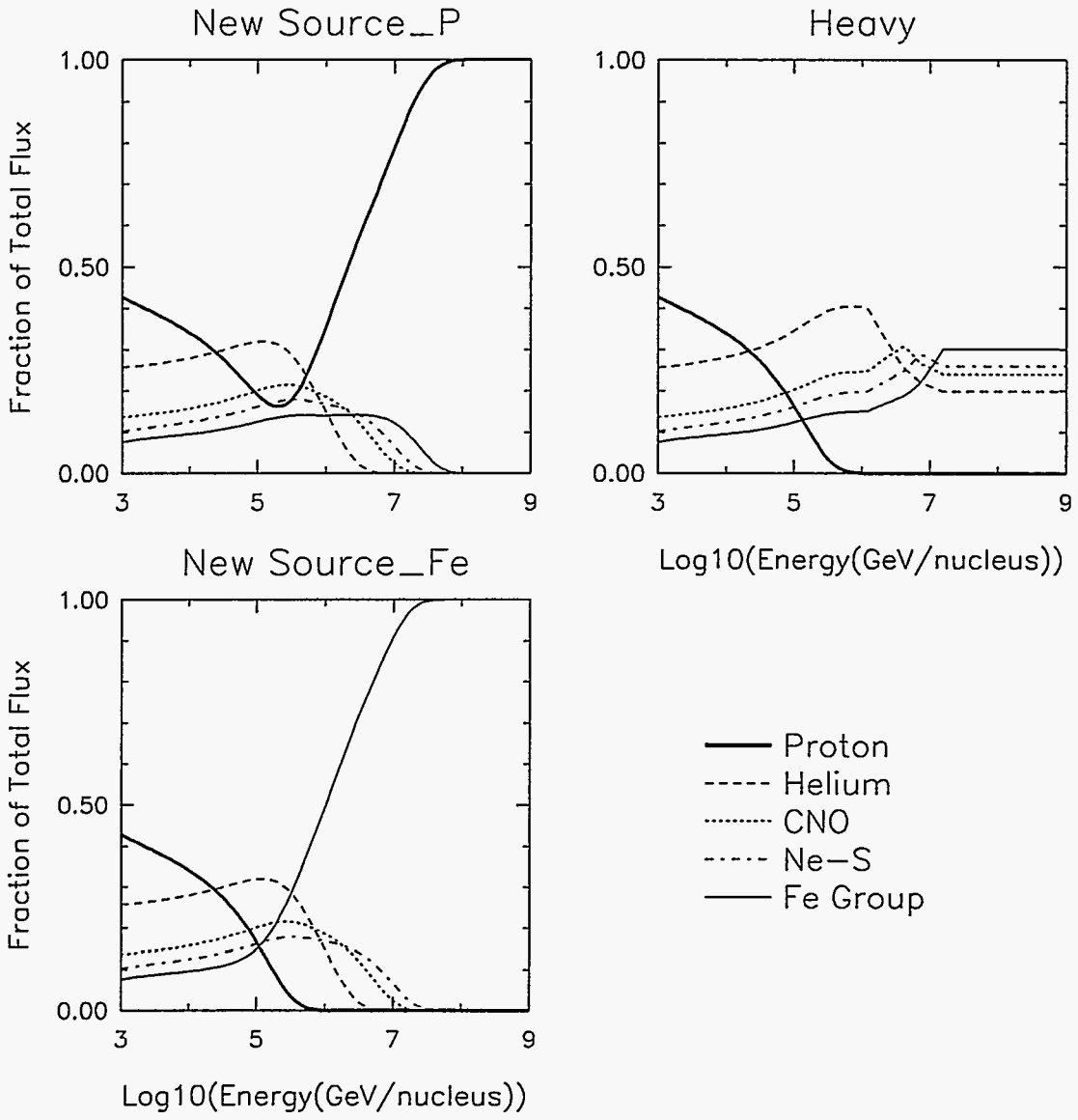

Figure 14: Energy dependence of the fractional compositions of the three models of cosmic-ray composition used to analyse Soudan 2 multiple muon data.

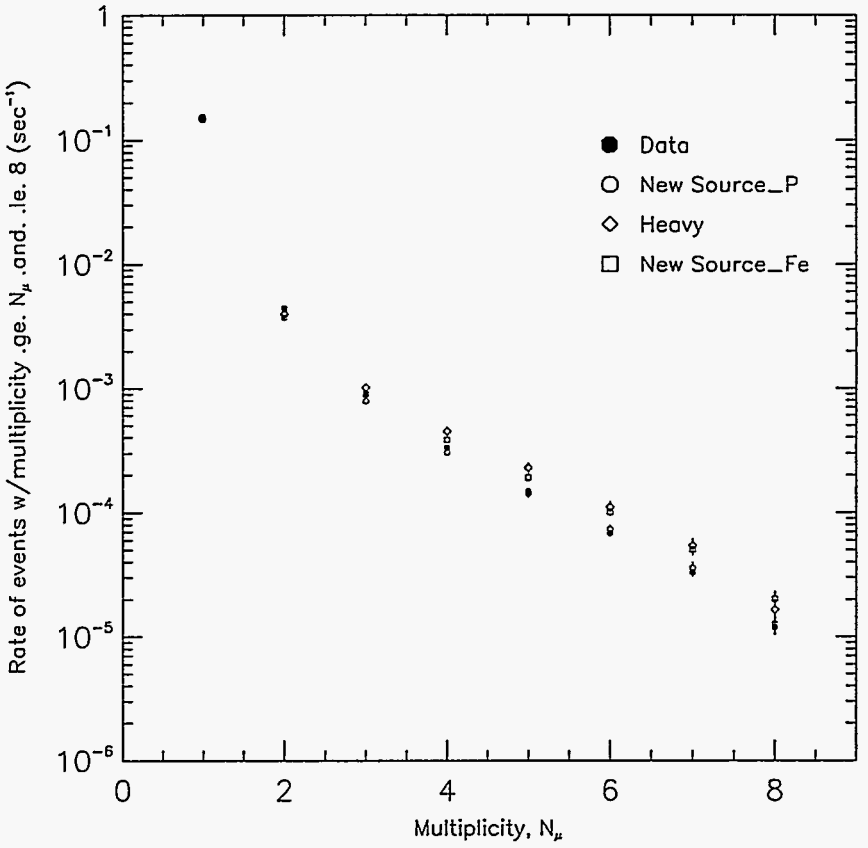

Figure 15: Comparison of Soudan 2 multiple muon rates with simulations based on the three models of cosmic ray primary composition shown in the previous figure. These preliminary results may eventually be extended to slightly higher multiplicities (corresponding to higher primary energies, and covering more of the "knee" region) as systematic effects associated with large-event data acquisition and reconstruction are better understood.

Argonne physicists continued to make substantial contributions to the maintenance and operation of the detector. Major activities included the ongoing study of detector and electronics performance, and coordination of the detector upgrade project. Argonne physicists are also continuing the development of software to make use of the dE/dx information from the detector.

c. Summary of Active Data Acquisition

The Soudan 2 detector is operated continuously for physics data whenever other activities permit. In practice, most data is recorded during night and weekend periods when installation or maintenance work is not in progress, and the underground laboratory is unoccupied. The anode-cathode edge trigger, which was devised for neutrino interactions and nucleon decay, has high efficiency for cosmic-ray muon tracks as well. All data are processed at Soudan by track reconstruction programs, and the analysis results are recorded on 8 mm magnetic tape cassettes for distribution to the collaborating institutions.

The Soudan 2 experiment continued routine data acquisition for contained events (neutrinos and nucleon decay) and cosmic ray muons during the first half of 1995. In addition, data from the 40 m^2 surface array were recorded in coincidence with Soudan 2 in order to measure the energies of some of the cosmic ray air showers which produce underground muon events. Data from a wide-angle air Cerenkov air-shower detector were also recorded in coincidence with Soudan 2 on clear moonless nights.

The Soudan 2 detector itself recorded data for 146 days of livetime, giving a duty cycle of 81%. This brought the total Soudan 2 exposure to 5.0 years, providing a total exposure of 2.4 fiducial kiloton years useful for nucleon decay and atmospheric neutrino physics.

d. Planning Activities

The upgrade of the North half of the detector is expected to be completed in the fall of 1995. At that time the North half of the Oxford crack filler array will be installed. During 1996, the active shield ceiling will be further enhanced by the installation of the last two "HPW" ceiling panels. Six of the eight panels of this array are already in operation. The HPW ceiling array uses proportional tubes from the HPW nucleon decay experiment to increase the detection efficiency for cosmic ray muons entering the Soudan 2 detector in the cracks between modules. The HPW tubes are oriented perpendicular to the original Tufts shield tubes in order to provide additional position information for cosmic ray muons. The two dimensional muon information is particularly useful for the reconstruction of multiple muon events in the active shield.

Soudan 2 experimenters also devoted a major effort to planning for the new MINOS long baseline neutrino oscillation experiment, which is described elsewhere in this report. During the first half of 1995, several major documents, including the MINOS P-875 Proposal, were prepared and submitted to the Fermilab Physics Advisory Committee and to the HEPAP Subpanel on Neutrino Oscillation Experiments. Argonne physicists played major roles in the planning for MINOS and in the preparation of these documents.

(D. Ayres)

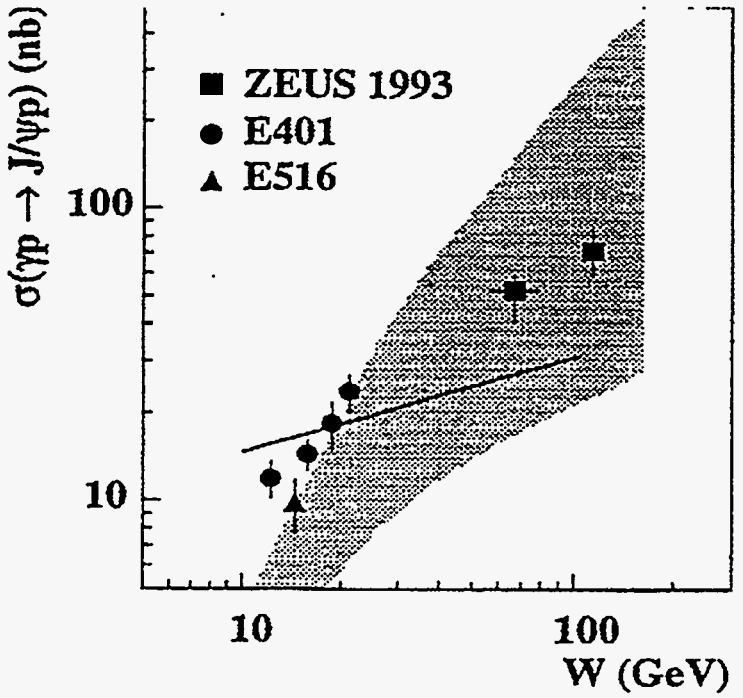

Figure 16: J/ψ elastic cross sections in photoproduction. The shaded region represents the prediction of the Ryskin model using upper and lower limits of the gluon momentum density extracted by the ZEUS experiment. The solid line is a VDM-like prediction.

I.A.5 ZEUS Detector at HERA

a. Physics Results

Twelve papers were published in this period and a further six manuscripts were submitted for publication.

In the continuing search for new phenomena a search for excited states of the standard model fermions was reported based on 0.55 pb^{-1} of luminosity taken in 1993. No evidence was found for any resonant state decaying into a fermion and a gauge boson. Limits on the coupling strength times branching ratio, for masses in the range from 50 GeV/c^2 to 250 GeV/c^2, were presented.

Measurements of the cross section for elastic J/ψ production in the reaction $\gamma+p \rightarrow J/\psi+p$ are used to study the reaction mechanism. Cross sections of $52^{+7}_{-12}\pm10$ nb at a c-m energy of 67 GeV and $71^{+13}_{-20}\pm12$ nb at 114 GeV were measured. The J/ψ particles were identified in their e^+e^- and $\mu^+\mu^-$ decay modes. The p_T ^{2} distribution has an exponential slope of 3.7 ± 1 GeV^{-2}. Figure 16 shows the ZEUS cross sections compared to lower energy data. The line which falls below our data points is the expectation from Vector Meson Dominance. The shaded area is the prediction of the two gluon exchange model of Ryskin using the upper and lower bounds of the gluon momentum density in the proton as determined from our F_2 values.

A related study reports the first cross section measurements, at HERA energies, for open charm production in $\gamma-p$ collisions. The charm particles were observed in the classical $D^* \rightarrow D\pi$

decay mode. The mass plots are shown in Figure 17. The total charm cross section is rising strongly with energy as shown in Figure 18. The lines are the NLO QCD calculations for different assumptions about the photon and proton structure functions.

Further jet studies were reported both in photoproduction and in Deep Inelastic Scattering (DIS). Dijet production in $\gamma - p$ collisions can proceed either through the direct coupling of the photon to a quark-antiquark pair or through a resolved component of the photon as shown in Figure 19. Previous ZEUS studies have shown that these two components can be roughly separated by a cut on x_γ at 0.75. The direct contribution is sensitive to the gluon content of the proton and the resolved contribution to the gluon content of the photon. The differential cross section $\frac{d\sigma}{d\eta}$ for dijet production with $E_T > 6$ GeV, the jets being selected with a cone algorithm, is shown in Figure 20 for the direct component. The same data is shown in all four plots and compared to several different calculations.

A classical measurement of the strong coupling constant is to compare the rate of di-jet production in DIS with next-to-leading order (NLO) calculations. This is most conveniently done using effective mass algorithms to do the jet counting. Before comparing the measured jet rates to the NLO calculations many effects must be understood; in particular, the collinear singularities. In addition, the reconstruction of forward going jets near to the forward beam pipe is particularly difficult. The latter point is illustrated in Figure 21 which shows the pseudorapidity distribution of the 2+1 jet sample (the 1 refers to the proton remnant) for the high Q^2 range of $160 < Q^2 < 1280$ GeV^2. The jets were selected with the JADE algorithm. The histogram shows the expectations from the ME and MEPS Monte Carlo simulations.

The two jet kinematics are defined by

$$x_p = \frac{Q^2}{Q^2 + \hat{s}},$$

where $\hat{s}$ is the square of the two jet effective mass, and

$$z = \frac{P \cdot p_{\text{jet}}}{P \cdot q} = \frac{1}{2}(1 - \cos\theta^*_{\text{jet}}),$$

where θ^*_{jet} is the polar angle of the jet in the γ^*-parton c-m system. The distribution of events in the $x_p - z$ plane is shown in Figure 22. The singularities at high and low z values are clear. The corresponding two jet rate is compared to two NLO calculations in Figure 23 as a function of the y_{cut} variable. The excess of the data over the calculations at low values of y_{cut} is due to the collinear singularities. With the larger data set available in the 1994 running reasonable event statistics remain after these regions are removed.

Charged particle multiplicities and momentum spectra were measured in the current region of the Breit frame. In this region, the characteristics of the quark fragmentation are expected to be similar to e^+e^- annihilation. This was indeed found to be the case as shown in Figure 24 which compares our measured mean charged particle multiplicity with one half of those from e^+e^- at the same Q values.

Figure 25 shows the variation of the position of the peak in the fractional momentum spectrum, $x_p = 2p/Q$, as a function of Q both for the ZEUS data and e^+e^- data. The full line, which agrees with the data, is the expectation from models in which coherent gluon radiation depletes the low momentum region. The dotted line is the phase space result.

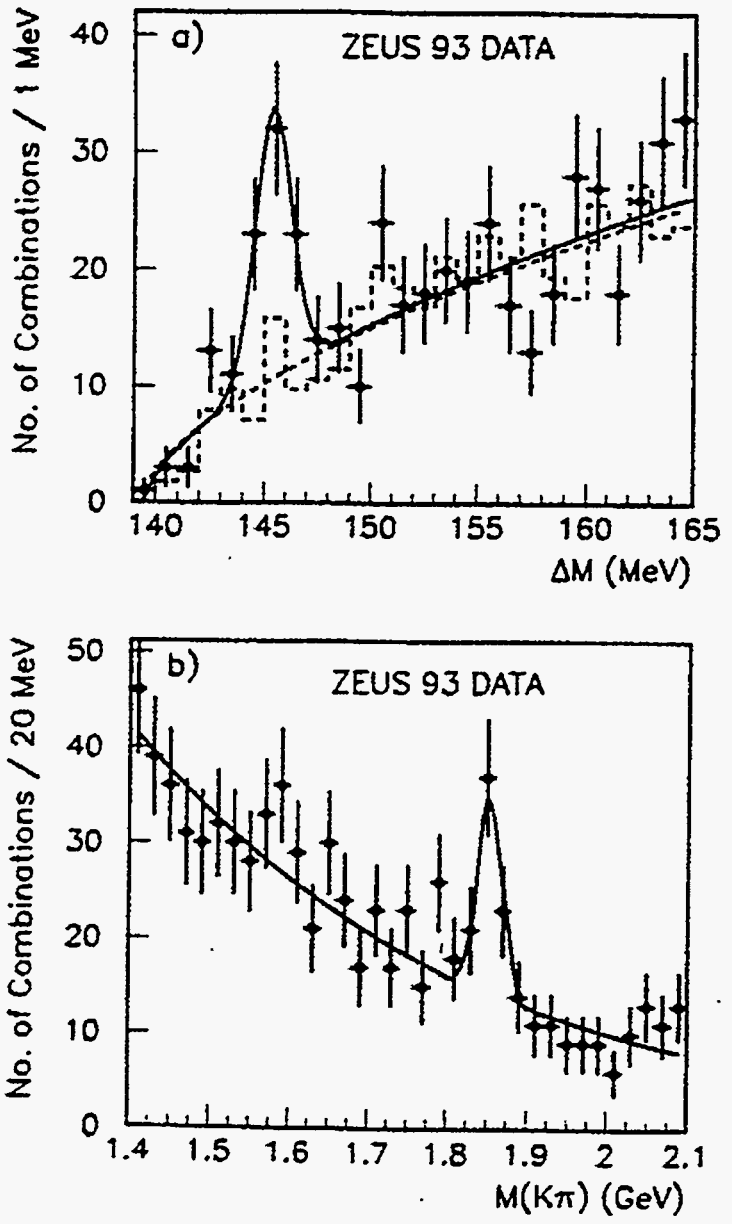

Figure 17: a) ΔM distribution for photoproduction events having $1.80 < M(K\pi) < 1.93$ GeV/c^2. The data are shown as points, the wrong sign charge background parametrization is shown as the dashed histogram, and the solid line is a fit to the distribution. b) $K\pi$ invariant mass distribution for candidates with $142 < \Delta M < 149$ MeV/c^2. The solid line is a fit to the data.

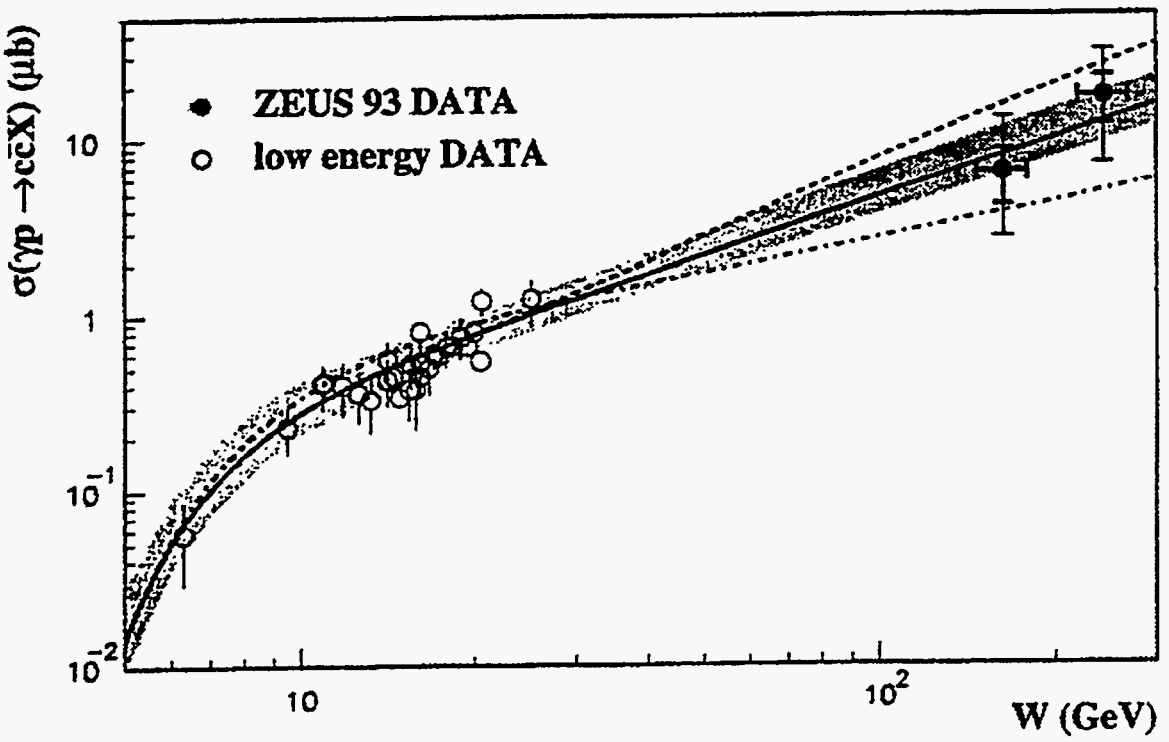

Figure 18: The total charm production cross section as a function of W. Solid line is the central prediction of NLO calculations and shaded band is the theoretical uncertainty from variation of the renormalization scale. The dashed and dash-dotted lines represent different choices of structure functions.

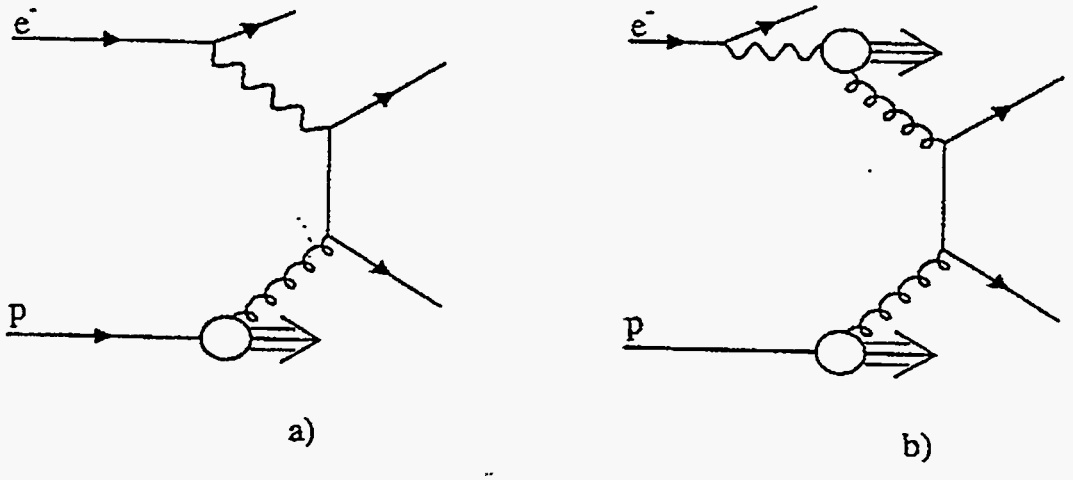

Figure 19: Examples of leading order diagrams for a) direct and b) resolved photoproduction.

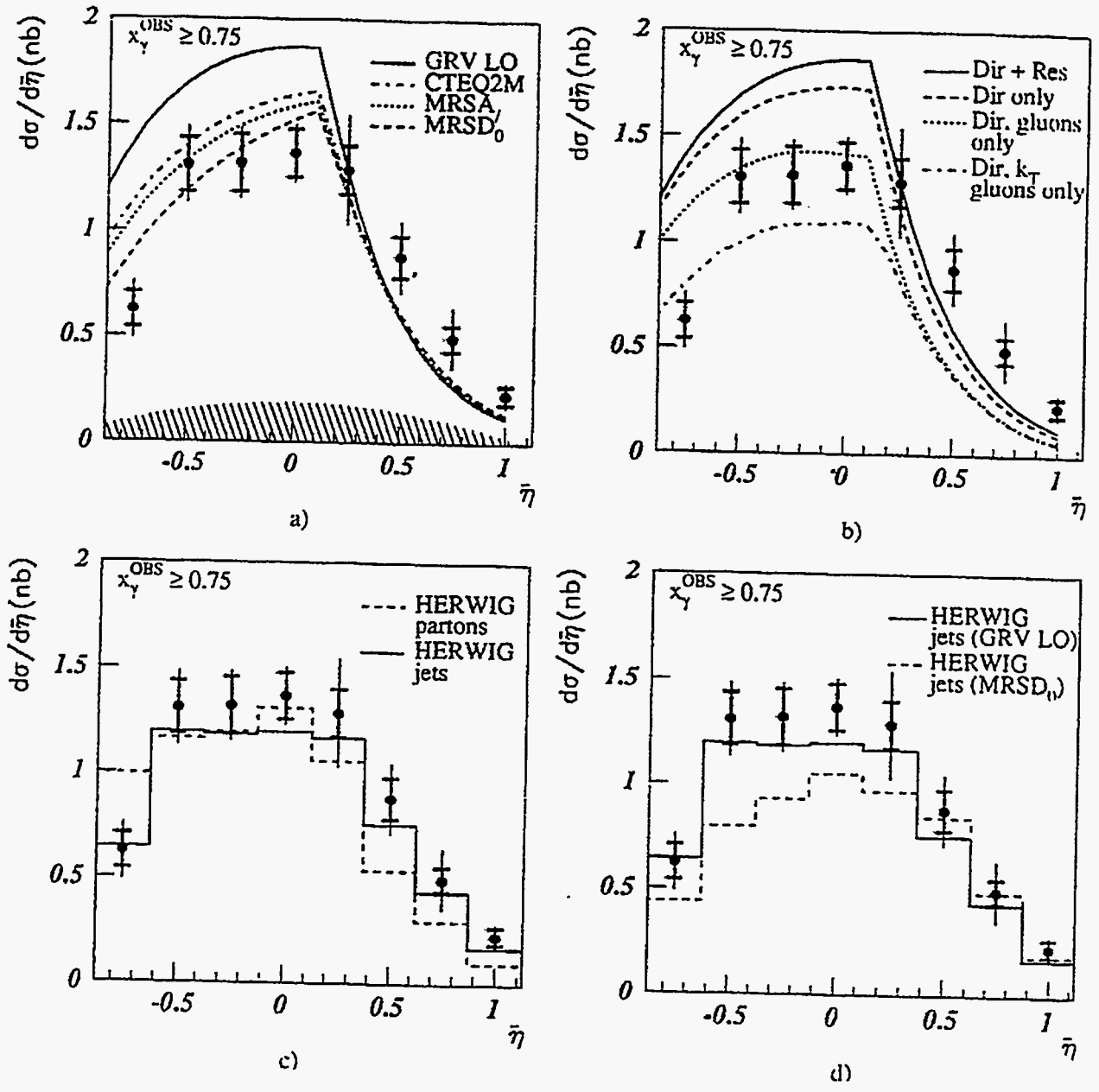

Figure 20: $d\sigma/d\bar{\eta}$ for $ep \to eX+ \geq$ 2jets. Solid circles are corrected ZEUS data. a) Data compared to LO QCD calculations for several parton distribution sets for the proton and the GS2 set for the photon. b) Similar to a) but with gluon processes as denoted. c) Data compared to HERWIG Monte Carlo estimates using partons and final state jets. d) Similar to c) using parton distribution sets as noted.

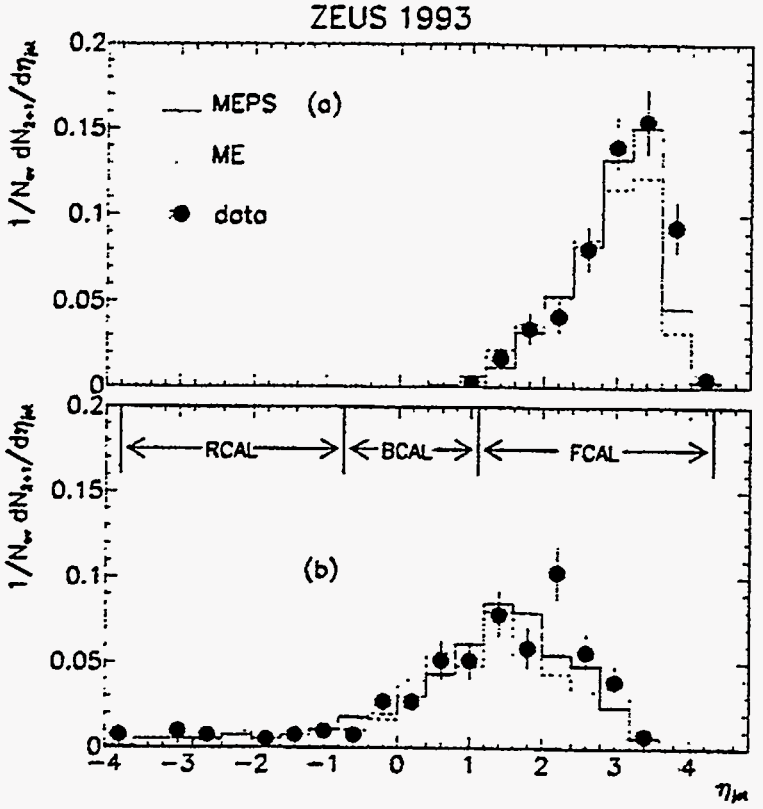

Figure 21: Pseudorapidity, η_{jet}, of the two jets in kinematic ranges $160 < Q^2 < 1280$ GeV^2, $0.01 < x < 0.1$, and $0.04 < y < 0.95$. a) Higher η jet. b) Lower η jet.

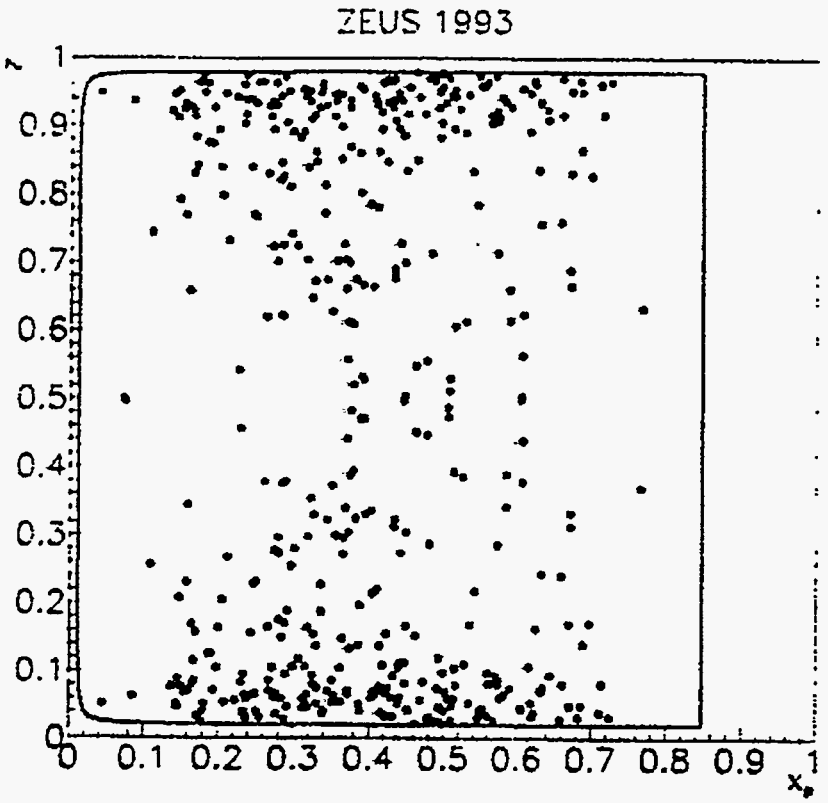

Figure 22: Distribution of z vs. x_p for uncorrected data in the high (x, Q^2) interval.

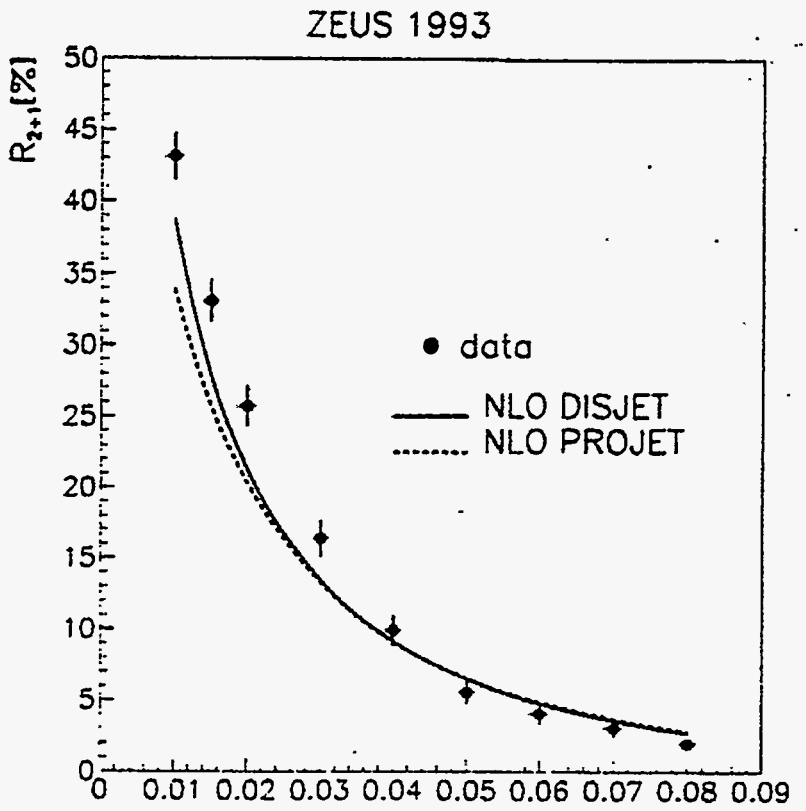

Figure 23: The corrected two-jet production rate R_{2+1} in percent as a function of y_{cut} compared to NLO calculations.

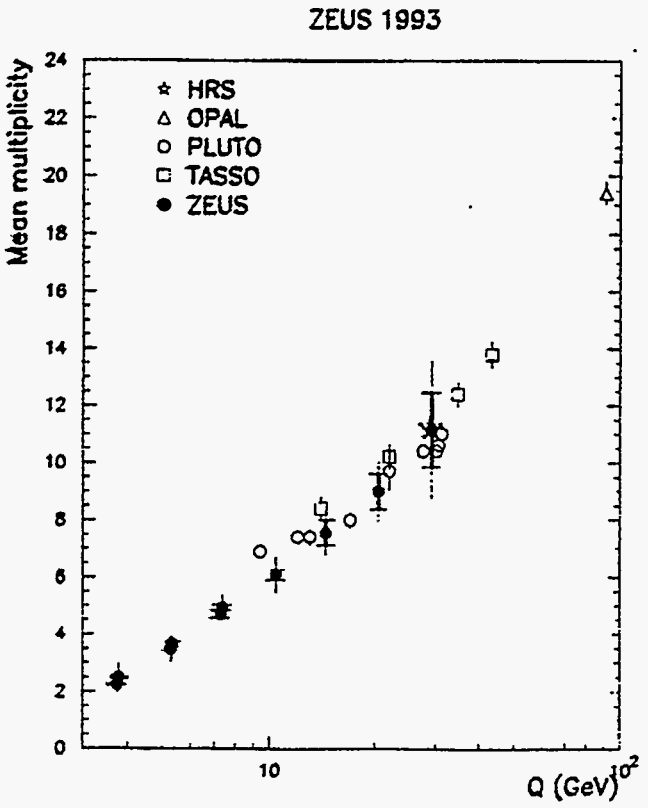

Figure 24: Mean charge multiplicity as a function of Q. Twice the measured ZEUS multiplicity is compared to results from various e^+e^- experiments.

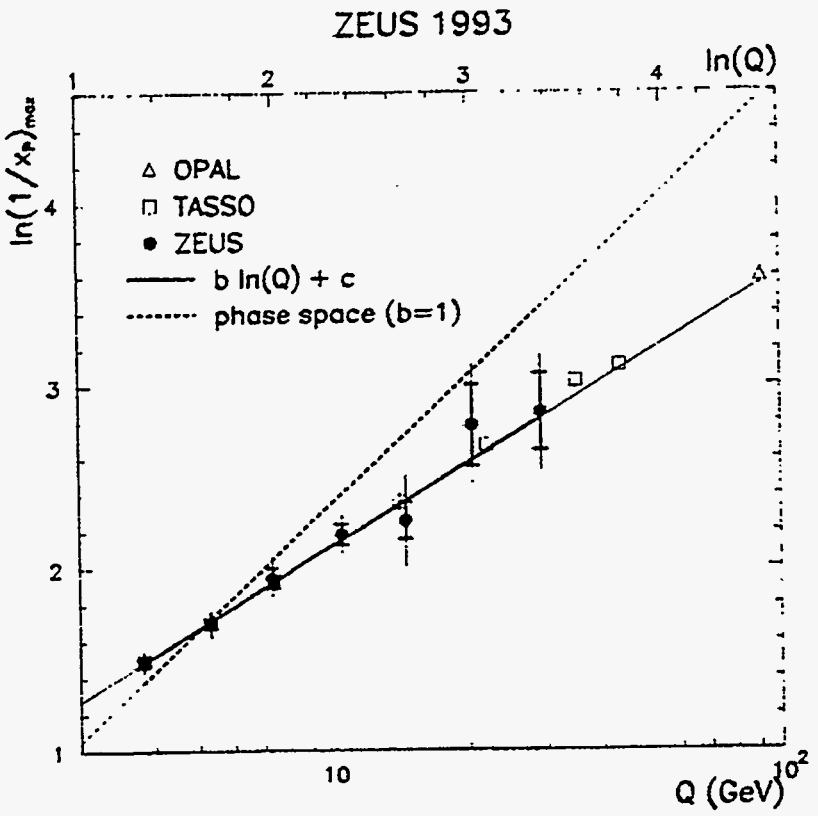

Figure 25: Variation of the peak of the fractional momentum spectrum as a function of Q.

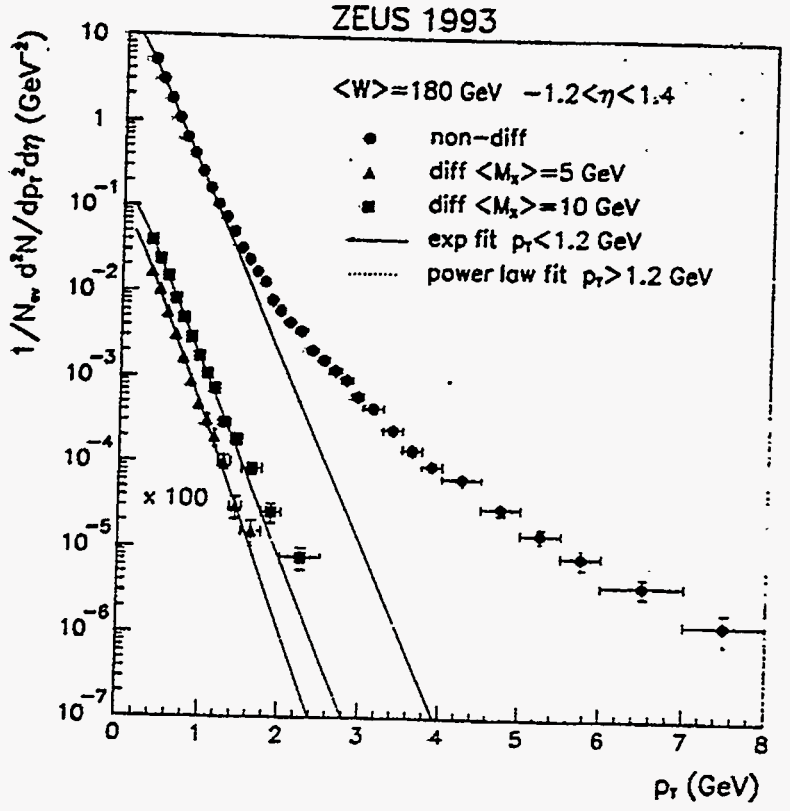

Figure 26: Inclusive p_T distributions of charged particles in photoproduction events at $< W > =$ 180 GeV averaged over $-1.2 < \eta < 1.4$.

A second study using the central tracking chambers measured the inclusive transverse momentum spectra in photoproduction for both diffractive and non diffractive events. The result is shown in Figure 26. The non diffractive data exhibits a clear excess at high p_T over an exponential — a characteristic sign of QCD activity. This is not the case for the diffractive data which indicates little gluon radiation for these events which have a low effective mass. The comparison with the NLO calculations of Kniehl and Kramer is shown in Figure 27. The agreement is good within the theoretical uncertainties of the calculation which is shown by the shaded band.

(M. Derrick)

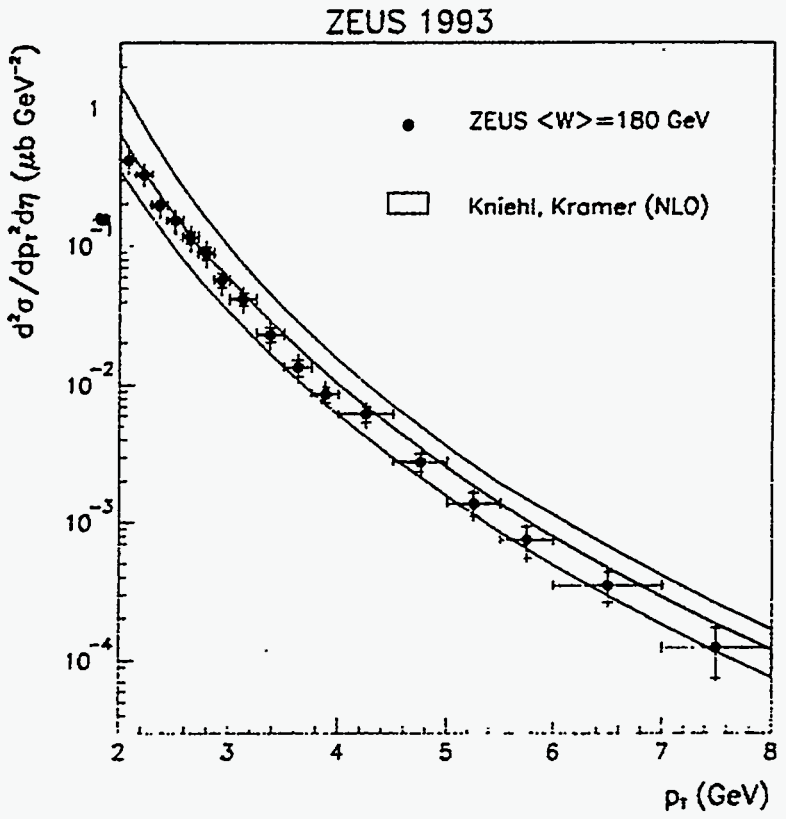

Figure 27: Comparison of ZEUS inclusive cross sections for non-diffractive photoproduction at $< W_{\gamma p} > =$ 180 GeV with a NLO QCD calculation.

I.B EXPERIMENTS IN PLANNING OR CONSTRUCTION PHASE

I.B.1 STAR Detector for RHIC

One of the major events occured in April when BNL Director, Nick Samios, organized a review committee to meet June 5-6 to look at the proton spin at RHIC and review the RHIC spin physics program. The committee, chaired by Charles Prescott, consisted of seven members. Although RHIC spin physics (R5) was approved by BNL PAC in 1993, many additional studies on the proposed measurements are needed. It was timely to examine many aspects of experiments for this review. Prescott and the committee concluded with a very positive attitude toward the spin program.

Earlier, we had the RHIC polarized proton review. This was a follow-up to a similar reveiew on June 21-22, 1993. This committee, assembled by Mike Harrison, consisted of the following members: Des Barber (DESY), Alex Chao (SLAC), Bob Pollock (IUCF), and Lee Teng (Chair, ANL). The committee met on March 16-17, 1995 at BNL. Their overall impression of the progress made on this project since the last review in 1993 was very positive.

The electromagnetic calorimeter meeting was held March 31 to April 1, 1995. One of the primary purpose of this meeting was to choose among the cast, stacked, and compressed options for the calorimeter module construction. The compressed option was chosen.

The RHIC spin collaboration meeting was held at MIT on May 7-8, 1995. The keynote speaker, Bob Jaffe, discussed important physics issues at RHIC. The status of RHIC spin, PHENIX, and STAR was extensively discussed by several speakers. The funding situation in general as well as RSC-STAR-PHENIX were reviewed.

Our measurements involve the detection of direct γ, jets, $W^{\pm}$ and Z° production in pp interactions. Here we describe various studies, some which were already complete, and others which are to be made in future. (A key person for the following studies is K. Shestermanov, an ANL visitor from IHEP, Protvino, Russia)

a. Efficiency of Jet Finding

The HIJING event generator (2 scattered partons), PYTHIA, and JETSET were used for event simulation. Initial conditions and kinematics of events are

- $\sqrt{s} = 200$ GeV
- p_T of the scattered parton = 30 GeV
- $\eta_{\min}$ and $\eta_{\max}$ for high p_T partons, $-0.3 \rightarrow +0.3$.

The efficiency of two jet finding is defined as Eff = N dijets/N dipartons, where N dipartons are generated events with two high p_T partons. A cone type algorithm (3 parameters) was used; the tower threshold for the seed transverse energy wasE_T = 1.0 GeV, the jet cone radius in the η - ϕ plane was $R_0 = 1$, and the threshold for jet energy was $E_j = 5$ GeV. The efficiency of jet finding was $80 \pm 10\%$.

b. Efficiency of Electron Finding

This study includes matching EMC energy to the track momentum, and establishing the hit position of the electron in the EMC, SMD, and charged tracks from TPC. Using the EMC table,

the efficiency of electron (from the W decay) finding turned out to be about 60-70%. SMD is yet to be included in the GEANT file. The problem is ϕ cracks; about 7% of electrons from W decay are not detected in the EMC. We need to introduce a cut on the value of $E_{\rm dep}/p_{\rm tot}$, where $E_{\rm dep}$ is the energy deposited in the EMC, and $p_{\rm tot}$ is the total momentum from TPC.

Preliminary studies show that in 1000 generated $W \rightarrow e + \nu_e$ events in the EMC with $\mid \eta \mid < 1.0$ we have

1. Electrons in EMC with $E_{\rm T} > 10$ GeV — 929 events,
2. Charged tracks in TPC — 837 events,
3. Isolation cut — 827 events,
4. $\mid z({\rm EMC}) - z({\rm TPC}) \mid < 1.0$ cm — 779 events, and
5. $E_{\rm dep}/p_{\rm tot} > 0.8$ — 677 events.

(We could do a correction on the energy deposited in EMC if the track is close to the ϕ crack and then we do not need the last cut.)

c. Other Studies in Progress

- Efficiency of photon finding — no charged track in TPC, shower profile.
- Jet efficiency vs. $p_{\rm T}$.
- Efficiency of $W^{\pm} \rightarrow e^{\pm} + \nu_e$, $Z^{\circ} \rightarrow e^+e^-$ finding together with background calculation.
- Background from $W \rightarrow \tau\nu_\tau$, $Z^{\circ} \rightarrow \tau^+\tau-$, where τs produce electron candidates, $\tau \rightarrow \nu_\tau e\bar{\nu}_e$.

d. Finding Z° in $Z^{\circ} \rightarrow$ jet + jet decay?

The branching ratio for $Z^{\circ} \rightarrow e^+e^-$ is 3.366% and for $Z^{\circ} \rightarrow$ hadrons is 69.90%. Reconstruction efficiency of both cases are compared — hadrons have a very wide spectrum causing a greater background.

e. $h_1(x)$ Measurements

Comparison of $h_1(x)$ measurements in $pp \rightarrow Z^{\circ} + X$ at 500 GeV and $pp \rightarrow$ jet + jet at 200 GeV were made. For simplicity, one flavor is dominant in the $h_1(x)$ measurement:

- $A_{TT} = a_{TT}(h_1/q)(\overline{h_1}/\overline{q})$ in Z° production,
- $A_{TT} = a_{TT}(h_1/q)^2$ in jet-jet production.

a_{TT} for dijet production is considerably smaller than that for Z° production, but the event rates are much larger. Furthermore, we measure h_1^2 in jet-jet while $\overline{h_1}/\overline{q}$ term is in Z° production. If $\overline{h_1}$ is close to zero, we cannot measure h_1.

From jet + jet, we want $qq \rightarrow qq$, but jet-jet includes qq, qg, gg depending on the $p_{\rm T}$ value. We also need to investigate the $q\overline{q}$ contribution, where a_{TT} is much larger than that of qq.

By using the CTEQTM structure function, the cross sections of qq, qg, gg in $pp \to 2\,\text{jets}+X$ versus p_T were calculated including the geometrical efficiency. In this estimate, we choose a p_T region where Signal(qq)/BG$(qg+gg)$ is $\frac{1}{2}$ at $p_T > 25$ GeV/c, $\sqrt{s} = 200$ GeV. Here we have 538,000 qq events (100-day run). By considering ϕ and θ coverage, we have 135,000 useful events. By assuming $(h_1/q) = 0.3$ (nonrelativistic case $(h_1/q) = g_1$), we have $\Delta(h_1/q) = 0.3$.

In $pp \to Z^\circ + X$ at 500 GeV, for simplicity, we assume $h_1/q = 0.3$ and $\overline{h_1}/\overline{q} = -0.3$. $a_{TT} = -1/\pi$ (see X. Ji, Phys. Lett. **B284**, 137 (1992)). We have 1350 useful Z° events and then $\Delta A_{TT} = \frac{2}{\sqrt{1350}} = 0.05$. For simplicity, let $\Delta h_1/q = \Delta\overline{h_1}/\overline{q}$, then we obtain $\Delta h_1/q = 0.3$. We will have $h_1/q = 0.3 \pm 0.3$.

(A. Yokosawa)

I.B.2 Main Injector Neutrino Oscillation Search: MINOS

The Soudan group, which previously had been working on a proposal for a Fermilab neutrino oscillation experiment (P822) using Soudan 2, has joined a new collaboration to build a large new detector in the Soudan mine to study neutrino oscillations. The collaboration includes Argonne, Boston College, Caltech, Columbia, Fermilab, Houston, Indiana, ITEP, Lebedev, Livermore, Minnesota, Oak Ridge, Oxford, Rutherford, Stanford, Sussex, Texas A&M, Tufts, and Western Washington. The MINOS Collaboration proposes to conduct a search for $\nu_\mu \to \nu_\tau$ and $\nu_\mu \to \nu_e$ oscillations using a new ν_μ beam from the Fermilab Main Injector with energies well above τ production threshold. Oscillations will be detected by the comparison of signals in a "near" detector at Fermilab and a "far" detector situated 730 km away. A new 10 kton detector will be built at Soudan to allow the exploration of oscillation parameters down to $\Delta m^2 \approx 0.002\ eV^2$ and $\sin^2(2\theta) \approx 0.01$. In addition the existing, much finer grained but smaller, Soudan 2 detector will provide an independent check of any potential signal with $\sin^2(2\theta)$ larger than ≈ 0.1.

In mid-1995, a HEPAP subpanel on neutrino oscillations, chaired by Frank Sciulli, compared the capabilities of the Fermilab MINOS experiment with a long baseline proposal at Brookhaven (BNL889). The subpanel's recommendation was that MINOS should be supported and that BNL889 should not. They gave three reasons:

1. The combination of MINOS with COSMOS, a short baseline experiment in the same neutrino beam, will be cost effective;
2. MINOS will have higher event rates, a larger variety of signals, and the possibility of a Narrow Band Beam (NBB);
3. MINOS will have greater "discovery potential" for $\Delta m^2 < 0.02\ eV^2$.

The discovery potential was defined by the subpanel as the region of parameter space in which one signal has 99.9% CL or greater and a second signature has 95% CL or greater. Each experiment was asked to show its discovery potential. This calculation depended crucially on a full understanding of systematic errors in all tests. It quantitatively depended on the power of the second best test. The MINOS discovery potentials for $\nu_\mu \to \nu_\tau$ and $\nu_\mu \to \nu_e$ are shown in figures 28 and 29. For $\nu_\mu \to \nu_\tau$, three curves are shown for differing assumptions about the systematic error for the disappearance signature.

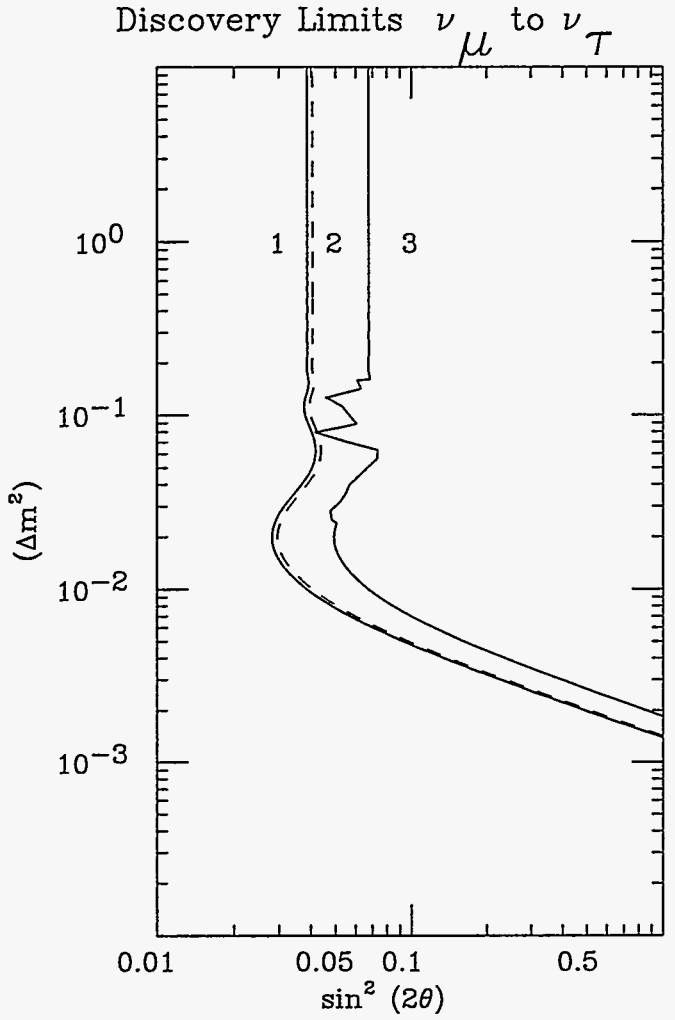

Figure 28: MINOS two year "Discovery level curve" for $\nu_\mu \rightarrow \nu_\tau$ oscillations. Discovery level is defined to be 99.9% CL in one test and 95% in a second test. The three curves shown differ by the assumption of systematic error. The curve to left is for no systematic error. The middle curve shows the range of parameters using our present estimate of systematic errors, which is 1% for the near/far test. The curve to the right shows the parameter space using a more pessimistic assumption of 2%. For parameter space to the right of each curve, we would be able to discover $\nu_\mu \rightarrow \nu_\tau$ neutrino oscillations with confidence levels greater than the specified values.

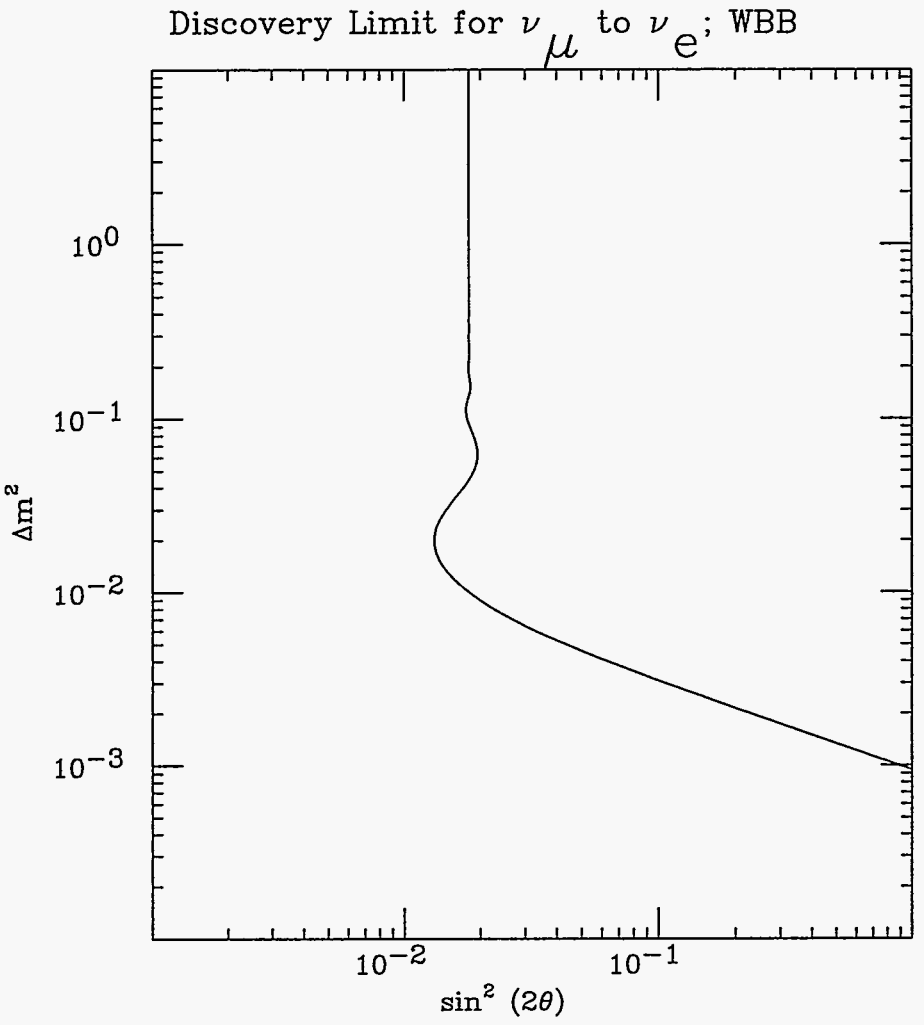

Figure 29: Discovery limits, as defined previously, for $\nu_\mu \rightarrow \nu_e$ oscillations.

The MINOS proposal describes a 10 kton reference detector which can be built using well understood technology. It will be built in a new hall at the Soudan mine, adjacent to the existing hall containing the Soudan 2 detector. The detector is designed to obtain measurements of muon momentum by range and/or curvature in magnetized steel, and to provide calorimetric measurements of hadronic and electromagnetic energy. The reference detector is a 36 m long, 8 m diameter sandwich of 4 cm thick octagonal steel plates separated by 2 cm gaps containing the active detectors. A total of 600 such planes constitute the mass of 10 kton. A coil running through a central hole will produce a toroidal magnetic field of $\sim$ 1.5 Tesla. The active detector elements will be 1 cm thick, 1 cm pitch limited streamer tubes.

Argonne has undertaken an R&D program in three areas for the MINOS detector. A limited streamer tube development program is underway to study the ideal geometry and the suitability of differing gas mixtures; and to provide a basis for mass production cost estimates. An electronics development program is determining the requirements for the 480,000 channels of electronics. A steel and magnet development program is involved in determining the optimal configuration of the passive detector vis-a-vis magnetic and structural considerations.

(M. Goodman)

I.B.3 ATLAS Detector Research & Development

a. Overview of ANL LHC Related R&D Programs

The first six months of 1995 have been a very busy period for the ATLAS detector development program. Early in this period the short range schedule for the production of full scale prototype modules was established (Figure 30). Although the actual schedule has slipped somewhat due to technical delays, it is still a challenging program. Argonne has responsibility for the design and development of the support girder, master plate fabrication via die-stamping, and the design and fabrication of the prototype stacking/compression table, all of which are critical elements early in this schedule. In addition, we have continued to work on the evaluation of surface characteristics relative to glue shear strength as well as on an evaluation of options for making the glue application semi-automatic. In support of this plan of distributed design, in this period, the TileCal group successfully established a network server for engineered CAD files and a news system on the World Wide Web to maintain current information and to provide rapid notification of design changes. We also established videoconferenceing for discussion of points of immediate concern and therefore this rather intensive, international design effort was monitored by only three engineering review meetings (held at CERN) in this period.

In conjunction with the mechanical design efforts, in this reporting period Argonne has contributed to the current TileCal test module test program, both by providing technical support for test module instrumentation and physicist effort in support of the testbeam data taking and analysis programs. In addition, we have continued scintillator component tests, in particular, with regard to the modification proposed by the Michigan State University group to use clear fiber welded to the wavelength shifting fiber in the tile readout.

The second general area of participation in the ATLAS experiment is in the design of the second level trigger supervisor. A pre-prototype trigger supervisor to test design ideas was designed in this period and is in the process of being fabricated and tested. This board will be tested in a high energy beam at CERN in September, 1995. Physics simulation studies of second level trigger

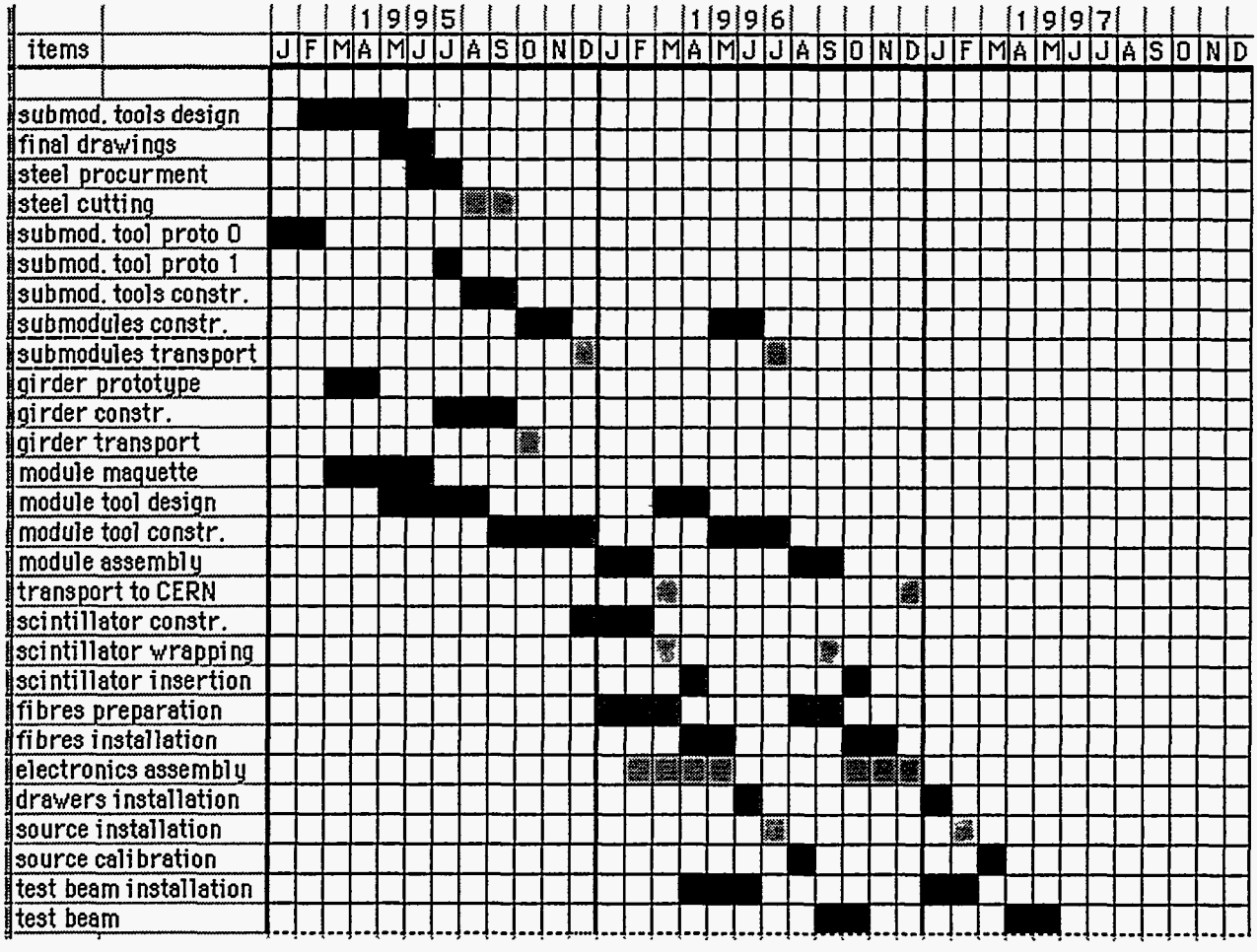

Figure 30: Initial schedule for the production and testing of full scale prototype modules for the ATLAS TileCal hadron calorimeter.

constructs were carried out and reported to the ATLAS electronics group and at an ATLAS physics meeting held at Trieste in June. These were received with considerable interest and will be pursued further.

An extensive discussion of R&D on the ATLAS TileCal calorimeter and on trigger electronics development and prototyping is found in the section covering detector development.

(J. Proudfoot)

b. Simulation Studies

Work has progressed in two areas of study in preparation for the involvement in the ATLAS LHC experiment. If the Higgs particle has a mass between 60 and 130 GeV/c^2 its detection will require spotting a very small resonance peak over a smooth background. Two methods have been identified for finding the Higgs in this mass range. One involves looking for a resonance in $b\bar{b}$ jets tagged in the ATLAS silicon tracker produced in association with a W or Z which decays to leptons. The Higgs will contribute to such events and the $b\bar{b}$ two jet mass should have a peak corresponding to the Higgs mass. CDF W plus jets data were used to check the methods being used to estimate backgrounds and mass resolutions for the ATLAS experiment by comparing the existing collider data to similar estimates. The comparison indicated that the methods are appear to overestimate the worst backgrounds (from W plus two jet events) at the Tevatron energies.

The other area that was explored was to compare the background rates for two photon events that are measured by CDF to the estimates made using the Pythia Monte Carlo. Pythia was used by ATLAS to evaluate the expected background for the two photon decay of the Higgs in the 60 to 130 GeV/c^2 mass range. The hadronic backgrounds, mostly pairs of isolated π°s or π° plus γ events, measured by CDF are higher than the Pythia prediction. The rate for prompt production of two photons is reasonably well modeled by Pythia. The implications of this for detecting the Higgs at the LHC still need to be understood.

(R. Blair)

I.C DETECTOR DEVELOPMENT

I.C.1 ATLAS Hadron Calorimeter and Trigger Development

a. Hadron Calorimeter Mechanical Design

The focus of the mechanical design work on ATLAS is now the production of full scale prototype modules for both the barrel and extended barrel regions of the detector. Argonne has primary responsibility for the design of the support girder, the stacking/compression fixture used in submodule assembly, master plate fabrication using die stamping and has taken a lead role in defining the plate surface preparation required for bonding. In addition, we are in contact with a robotics company here in the US to develop a possible design for a semi-automatic glueing fixture as we are concerned that the design being developed in Europe may not be as cost effective here in the US.

The following internal Technical notes and papers have been submitted during this report period:

1. Drawing Set for the Stacking Fixture (AT-310-1-0 Stacking Fixture Assembly & Parts List)
2. Technical Specifications for Plate fabrication for the ATLAS Tile Hadron Calorimeter, ANL-HEP-TR-95-39
3. Specifications for Steel Production (written by Marzio Nessi with edits by N. Hill), ATLAS Internal Note No. 51 May 26, 1995
4. Trip Report for trip to Steel Warehouse Inc. South Bend Indiana (internal memo), May 4, 1995
5. Thoughts on Steel Procurement (internal memo) April 24,1995
6. ATLAS Barrel Hadron Calorimeter Module Assembly and Tooling Design, ATLAS Internal Note TILE-CAL No. 52 May 26, 1995
7. Procedure For Stacking TileCal Submodules, ANL-HEP-TR-95-54
8. Report of Time Saver Surface Finish Tests, ANL-HEP-TR-95-55

i. Argonne Girder Design

The girder design was completed in January of this year here at Argonne and modified slightly in CERN to accomodate changes in the interface to the optical components. A prototype girder which followed this design was fabricated by the Bucharest group and met the specification. The design for prototype Barrel 0 module is now final.

ii. Master Plate Manufacturing

During this period the specifications for the necessary steel to construct the first full scale prototype TileCal module were written and edited. Argonne HEP engineers contributed to both the content and technical aspects of those specifications. An investigation of possible sources for the steel in the US was conducted and 7 potential sources were identified. One trip to a local steel

cold reduction facility was initiated and the information obtained. This increased our knowledge about the cold reduction process and the tolerances that could be achieved using this technique.

The masterplate drawing (AT31012) was revised at Argonne to make it compatible with both the ANSI and ISO standards. In addition, several minor revisions were made in early 1995 (the ears, radial dimensions and hole sizes were changed). This drawing is now maintained in the electronic files at CERN in both the CERN and ANL formats.

The steel procurement for the required master and spacerplates was initiated by CERN laboratory, and three European Companies plus three US companies were solicited. Due to some communication difficulties no reponses were received from the US vendors. The low bid was received from the Czech Republic company (Kralodvorske Zelezarny).

The Argonne engineering staff have for some time proposed that die stamping is likely to be a more cost effective approach for the fabrication of the master plates, since they have a complex pattern of holes and boundary and are required to be manufactured to a very high tolerance. We have, therefore, pursued this approach and have ensured that the design of the plate does not preclude die stamping for any simple reason. Stamping has the problem that the shearing action of the die causes a burr on the finished plate. This is unacceptable and we have, therefore, also investigated techniques whereby this burr may be simply and cheaply removed. The approach that we are proposing uses an abrasive belt to remove the burr without significantly removing material from the plate ("Time Saver" process). In addition, we propose that this process may be used to apply a surface roughness to the plates for glue adhesion. Test samples were prepared at the end of June and will be tested for bond strength in July. We do not anticipate any surprises and are confident that this method will be acceptable.

Familiarization trips were made to two die manufacturers and steel stampers in preparation for soliciting bids for the stamping of the large masterplates. A specification was written and approved for the manufacture of those plates. In an effort to make legitimate comparisons between proposed laser cutting and stamping prices, estimates for both techniques were obtained in the US.

iii. Stacking/Compression Table Design

After Argonne participation in the stacking of the first three test submodules at CERN, several items were noted that could be improved in any future designs for the assembly tooling. Argonne was given the opportunity to incorporate this knowledge into a new design for the stacking fixture. This fixture was designed and submitted to the mechanical group at the ATLAS week meeting in June. The design was accepted and approved for construction. Figure 31 illustrates the primary features of this fixture.

iv. Glue Application, Surface Testing and Bond Strength Measurement

A number of confirming tests were conducted at Argonne on the adhesive bonding of the plates, the surface preparation of the plates and an alternative fixture for doing the adhesive application on the submodules.

A set of bond tests were conducted early in this report period that were in accordance with the ANSI and ISO specifications. These tests confirmed results obtained with the adhesives specified for bonding the submodules. Argonne also proposed that since it was necessary to deburr the plates before bonding , that the deburring process could also be used to prepare the surface. It was proposed that a process developed by a US company named Time Savers could be used for

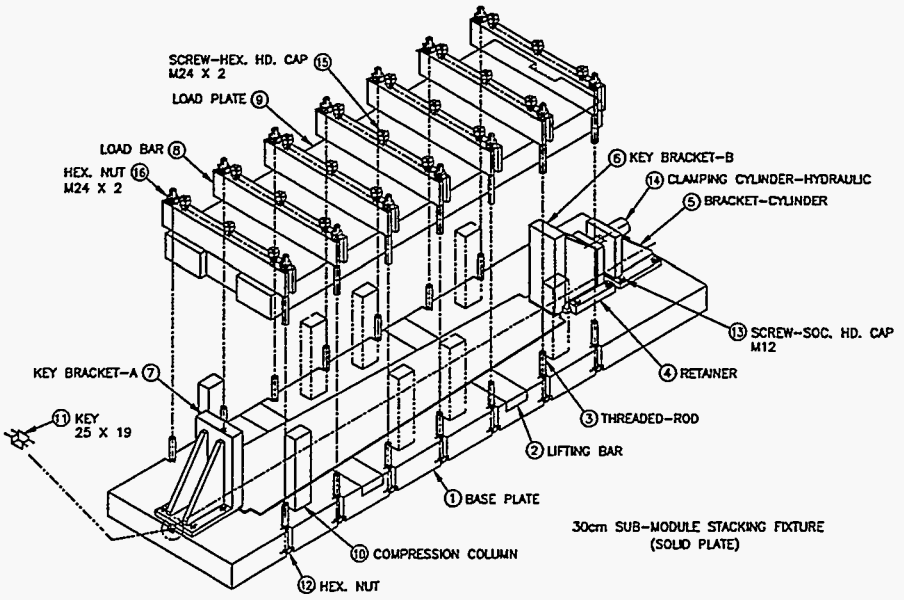

Figure 31: Stacking & compression fixture - schematic

both the deburring and surface finishing simultaneously. This proposal was tested, confirmed, and accepted for the production of both the master and spacer plates.

A proposal has been made to the TileCal collaboration that the current method of applying adhesive to the plates prior to bonding as a separate operation could be made less labor intensive and efficient by performing this operation on the stacking fixture. We have established contact with a commercial robotics system supplier and obtained a conceptual design and cost estimate for a system which may be integrated with the stacking table. This, as well as other options, will be investigated by the University of Illinois group in conjunction with Argonne.

(N. Hill & J. Proudfoot)

b. Scintillator Readout Design Tests

Several possible improvements to the TileCal optical system were being considered by the group in the 1995 testbeam program. These included the use of scintillator produced by an improved technique, the addition of quenching agent to the wavelength shifting fibers to reduce Čerenkov light and welding of clear fiber to the wavelength shifting fiber in order to reduce the overall signal attenuation. The effect of each of these changes was measured at the component level using the 3 MeV ruthenium source in the Division.

The light yield as a function of tile size was measured for the improved tiles. This is shown in Figure 32, where it is seen to fit well with the L/A scaling reported by CDF and SDC tests, where L is the length of wavelength shifting fiber coupled to the tile and A is its area. The attenuation lengths of clear and wavelength shifting fiber were measured to ensure consistency with earlier work

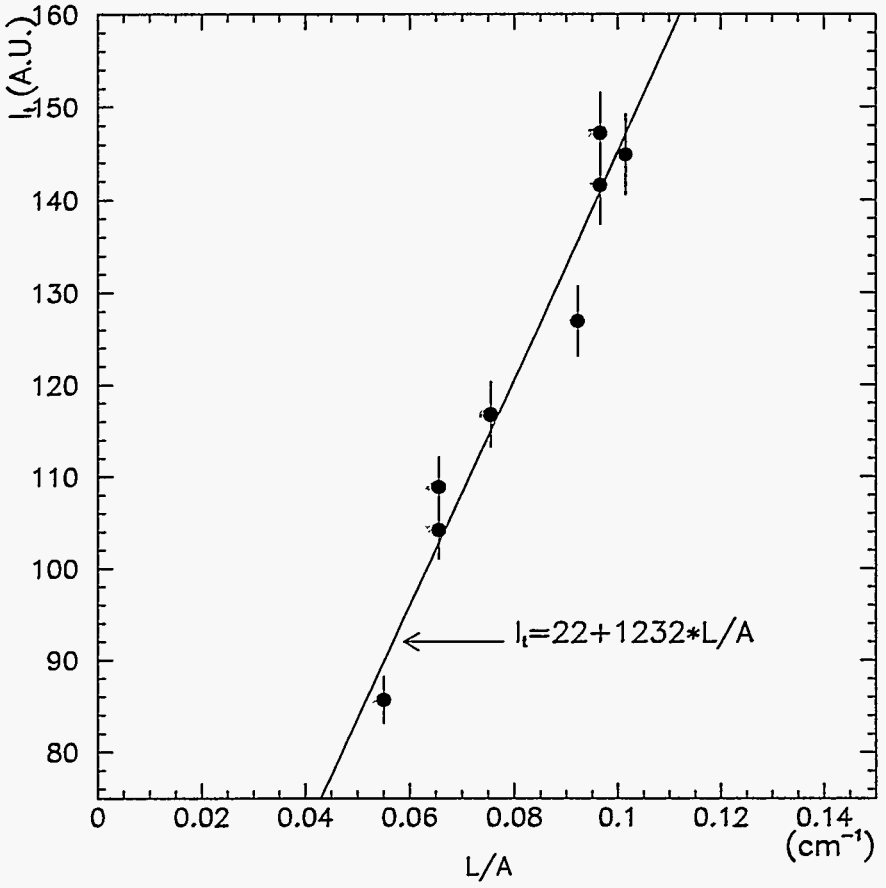

Figure 32: Tile response as a function of tile area for tiles used in the 1995 re-instrumentation of the TileCal test modules. The line shows a fit to L/A scaling, where L is the total length of wavelength shifter coupling to the tile (in this case 20cm) and A is the tile area (cm^2).

Tile ID	Tile Area A cm^2	Tile Relative Light Yield	Fiber Atten. Factor	Net Relative Response
1	226	0.89	1.00	0.89
2	236	0.86	1.04	0.89
3	246	0.83	1.08	0.90
4	333	0.80	1.13	0.90
5	349	0.77	1.19	0.92
6	366	0.75	1.24	0.93
7	442	0.72	1.31	0.94
8	465	0.69	1.39	0.96
9	487	0.67	1.47	0.98
10	649	0.64	1.58	1.01
11	684	0.62	1.69	1.05

Table 1: Optical model calculation of net signal as a function of tile number for tiles to be used in the barrel 0 prototype module when full length wavelength shifting fiber is assumed for the readout. The response is relative to tile ID 1 of the barrel test module.

and used to compute the expected gain in light yield of the WLS/green combination compared to a full length WLS fiber. Calculations using this data indicated that for the longest fibers, the WLS/clear system should give a gain of between 20 and 40% in light relative to a full length WLS fiber. Comparison of two sets of fibers from the two geometries showed the WLS/clear system to give a 10% loss of light. This outcome was unexpected, and later it was determined that a likely cause is the use of single rather than multiclad clear fiber.

The component characteristics have been used to develop a model for the tile-by-tile response of the test modules and for the Barrel 0 prototype module with some assumptions concerning the lengths of fiber required to route signals to their photomultiplier tubes. The calculated response in the prototype tiles (which have significantly different L & A characteristics relative to the test module tiles) is shown in Table 1. The net tile-to-tile response is expected to be quite uniform. However, this is a result of a cancallation of the decrease in tile signal with tile area with the decrease in signal attenuation along the fibers as tiles become closer to the outer radius. More study is required since at present L/A scaling has only been tested for tiles of about half the area of the maximum size tile in the ATLAS design and, in addition, the final fiber routing has not been defined.

In addition to the component measurements, analysis has also begun on measuring tile to tile variation in the 1995 testbeam data using the response of the calorimeter to 150 GeV muons impacting at 90° to the tile surface. These data will be used to compare to the component based model and to assess where more, if any, work is required in the optical system to achieve the uniformity required to realize the design resolution.

(J. Proudfoot)

c. Test Beam Program

Argonne again contributed in a substantial way to the support of the TileCal 1995 testbeam program. We have supported module construction, participation in shifts and data analysis.

Early in the design of the calorimeter modules, we suggested several modifications in the optics to improve the uniformity of the transverse response. One of these modifications included the addition of Tedlar strips to the edges of the scintillator tiles. Following up on this modification, we cut approximately 700 pieces of Tedlar strips of five different sizes and supplied these to European colloborators for inclusion in the tile wrapping process.

A technician was sent to CERN to assist in the assembly of two of the modules modified in 1995. We supplied two weeks of effort in wrapping and inserting scintillator tiles, and routing fibers from the tiles to the phototubes. As mentioned above, two staff members visiting CERN also assisted in the re-stacking effort.

In May, five modules were moved to the testbeam and the testbeam program was continued with one of the goals being the understanding of the improvements made to the two modules re-stacked in 1995. These two modules used an improved batch of polystyrene-based injection molded scintillator tiles appropriately masked with the Tedlar strips. Furthermore, the tiles in all the modules were read out using a variety of fibers. Improvements to the 1995 modules included the use of Y11 multiclad fibers with UV absorber. In addition, shorter Y11 fibers from tower 1 on each of these two modules were spliced to clear fibers for the routing to the phototube. Three Argonne physicists provided effort taking shifts during May and June.

We have continued our analysis of the data from the testbeam programs. In January we presented results of our analysis of the combined TileCal plus liquid argon run in September, 1994. We found that the response of the TileCal in this configuration was about the same as in the standalone configuration. In addition we showed that first, there was too much noise in the EMC calorimeter to give the purported resolution and secondly, that the total EMC plus HAC energy was not well understood because of beam scraping, transverse leakage, and/or bad liquid argon calibration.

The muon analysis presented at the June, 1995 ATLAS meeting centered on investigating the transverse uniformity of the tiles and the effect of the various fiber types. Scans show, in fact, that the transverse uniformity across the masked tiles is at an acceptable level compared to the testbeam runs of 1994. Also verified is the effect of UV quencher in the fibers. In figure 33 we see the enhancement of the signal in Module 2 where a BCF91A fiber was located. Other modules show no such enhancement.

(R. Stanek)

d. The ATLAS Level 2 Supervisor and Region-of-Interest Builder

Responsibility for the design, construction, and implementation of the ATLAS Level 2 Supervisor and Region-of-Interest Builder will be shared by Michigan State University (MSU) and Argonne. During the period Argonne and MSU have participated in a number of meetings organized to plan the level 2 trigger, and to define the responsibilities of the various participants. One of the outgrowths of these meetings has been a plan to run a set of prototype level 2 hardware in the ATLAS test beam in September, 1995. Argonne and MSU will provide the hardware and software for the prototype level 2 Supervisor for this test beam run and for laboratory tests which will be conducted at CERN on an ongoing basis. The hardware consists of a processor in VME using a TMS320C40 Digital Signal Processor, a purchased module, and a VME module designed and built by Argonne which receives region-of-interest information from beamline elements and performs various logical operations. The software will be a joint responsibility of MSU and Argonne. At the

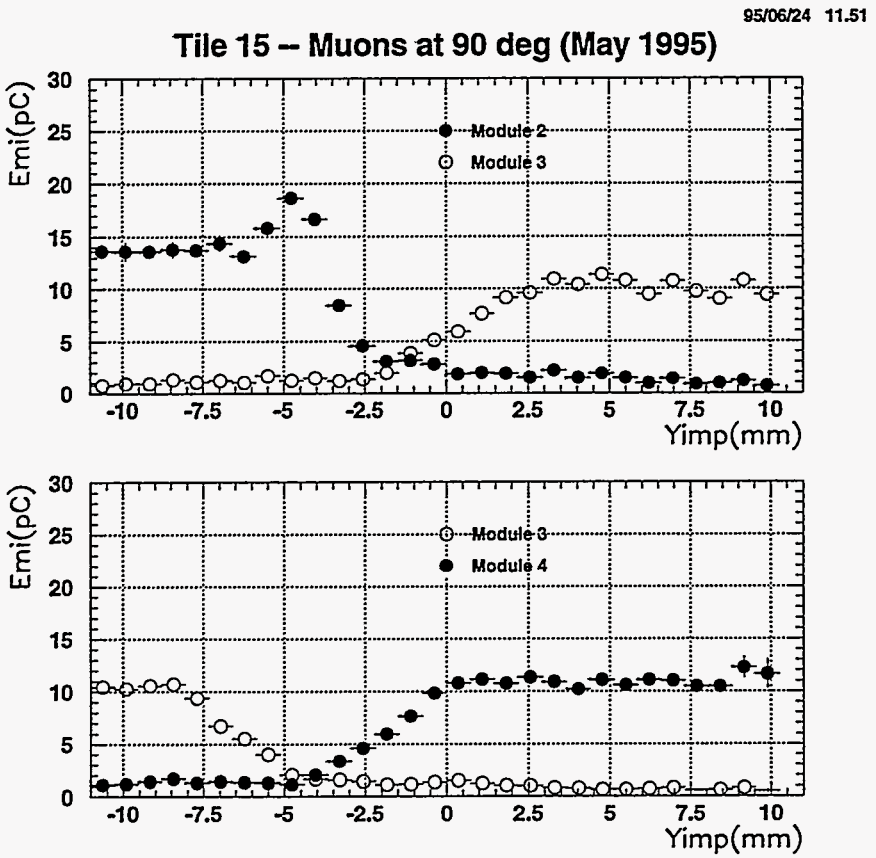

Figure 33: Response to muons near the edges of the scintillator tiles for Modules 2-4. The enhancement due to the BCF91A fiber is seen in Module 2. The transverse response across the tiles in Module 3 is uniform.

close of the period two prototype supervisors had been built and testing is proceeding.

(J. W. Dawson)

II THEORETICAL PHYSICS PROGRAM

II.A THEORY

II.A.1 Precise Calculation of the Cross Section for Top Quark Production

The quest for the top quark reached fruition recently with the publication of results by the CDF and D0 collaborations who studied $t\bar{t}$ pair production in proton-antiproton collisions at the Fermilab Tevatron: $p+\bar{p} \to t+\bar{t}+X$. The large mass of the quark and the possibility that its observed cross section exceeds theoretical expectations have, in turn, stimulated considerable theoretical activity. Edmond Berger and Harry Contopangos examined the quantitative reliability of calculations of the production cross section in perturbative quantum chromodynamics (QCD). They published a new calculation of the total cross section for top quark production based on an all-orders resummation of soft gluon radiative corrections to the basic perturbative QCD subprocesses. Their work is summarized in Argonne report ANL-HEP-PR-95-31, accepted for publication in *Physics Letters*, and in ANL-HEP-CP-95-51, an invited paper presented by Harry Contopanagos at the International Symposium on Theory and Phenomenology in Particle Physics held at Iowa State University in May, 1995.

At lowest order, the two partonic subprocesses that contribute to $t\bar{t}$ pair creation are quark-antiquark annihilation and gluon-gluon fusion. These subprocesses are of order α^2 in the strong coupling strength. Both order α^2 and the next-to-leading order α^3 contributions have been investigated thoroughly in the past. One observation is that the $O\left(\alpha_s^3\right)$ terms in the partonic cross sections are particularly large near the $t\bar{t}$ production threshold. This region of phase space is important for top-quark production at the Tevatron, owing to the large mass of the top quark. The large threshold corrections can be identified with numerically large logarithmic terms attributable to initial-state gluon bremsstrahlung. When large logarithmic contributions are present, their resummation to all orders in α_s is important both for theoretical understanding of the perturbative process and for numerical control of the resulting predictions. Berger and Contopanagos use the "principal value resummation" method to include all large threshold corrections. This method is free from arbitrary infrared cutoffs; the Landau poles in the running coupling strength are by-passed through a Cauchy principal-value prescription. This constitutes a theoretical advantage in comparison with an earlier, and oft-cited, resummation calculation of the top-quark cross section, for which dependence upon an undetermined infrared cutoff was explicit. Another related and important advantage is that the method permits an unambiguous, parameter-free specification of the region in subenergy in which perturbative resummation is applicable. Berger and Contopanagos completed a full resummation for the dominant quark-antiquark subprocess as well as for the glue-glue channel whose larger color factor introduces added complexity. For a top mass of 175 GeV, they compute a $t\bar{t}$ pair cross section at the Tevatron of $5.52^{+0.07}_{-0.45}$ pb, in respectable agreement with experiment.

(E. Berger and H. Contopanagos)

II.A.2 Prompt Photon plus Associated Heavy Flavor at Next-to-Leading Order in QCD

Edmond Berger and Lionel Gordon are engaged in an analytic calculation of prompt-photon plus associated heavy flavor production at large values of transverse momentum. They are working at

next-to-leading order in perturbative QCD. A draft paper summarizing some of their conclusions has been prepared, ANL-HEP-PR-95-36; it will be submitted shortly for publication. Most calculations of production processes in QCD have been calculations of the inclusive production of a single particle. Berger and Gordon are breaking new ground in performing a fully analytic computation of a *two-particle* inclusive distribution, with specification of the momentum variables of both the final prompt photon and the final heavy quark. Nine partonic subprocesses contribute at $O(\alpha_s^2)$. Berger and Gordon have computed all of these, along with the pertinent virtual-gluon-exchange terms, and analyzed their singularity structure, factoring initial-state collinear singularities into the appropriate initial parton densities, and final-state singularities into fragmentation functions. In their work, they found important modifications to expectations based on the lowest order, $O(\alpha_s)$, subprocess $gc \to \gamma c$. Their results will provide a new test of perturbative QCD and a means for measuring the charm quark density in the nucleon from hadron collider data being analyzed by members of the CDF collaboration. After completion of the analytic phase of this work, they have begun to produce a versatile Monte Carlo generator that will allow more differential comparison with data. Longer-range plans include a similar next-to-leading order calculation for polarized proton-proton scattering.

(E. Berger and L. Gordon)

II.A.3 Canonical Dual Transformations and Supersymmetry

In Phys. Rev. **D52** (1995) R573, Cosmas Zachos and Thom Curtright (Univ. of Miami) invented the Supersymmetric Dual Sigma Model (SDSM). This is an unexpected two-dimensional field theory to which the standard supersymmetric Chiral σ-Model maps under the canonical transformation found by these authors.

In the past, bosonization techniques transforming a local field theory nonlocally to an *equivalent* but very different-looking local field theory have provided efficient handles for better understanding the behavior of such systems. A canonical transformation is one which preserves Poisson Brackets (commutators and anti-commutators), and thus the functional measure and the overall quantum behavior of a model. The unique extant non-Abelian dual canonical transformation which connects two local bosonic 2d field theories to each other has been invented in the past by the same authors, but a systematic general theory is still lacking. Nevertheless, such transformations of fermions to fermions had not been investigated until the authors posited an *Ansatz* for the generating functional of a canonical transformation of the supersymmetric extension of the σ-model. (Supersymmetry was used as a crutch, since results on bosons were already available.) This informed *Ansatz* shed considerable light on the canonical transformation of fermions to fermions, for the first time. It involves a chiral rotation (on the tangent space of "pions") reflecting duality, in marked contrast to the bosonization of fermions.

As in the bosonic case, all currents (fermionic and bosonic) mix locally. But the boson fields now engulf fermions in the map: The purely bosonic curvature-free currents of the chiral model become a *symphysis* of purely bosonic and fermion bilinear currents of the dual theory. This is a novel field theoretic mechanism. The realization of supersymmetry in the SDSM is, in fact, a non-standard chirally-twisted one, and is dictated by the extraordinary geometry of the field manifold of the dual theory, which is also under investigation (in preparation). The full implications of this geometry on the renormalization of these models are currently being explored by the community, as well as by the authors.

Finally, in the same publication, it was argued that the transformation functional which relates wavefunctions in the two quantum theories (Dirac, 1933) be *exactly* given by the exponential of the generating functional introduced.

(C. Zachos)

II.A.4 Higher-order BFKL Evolution

The small-x evolution of parton distributions is described by the BFKL equation. Alan White obtained higher-order corrections to the BFKL equation by combining gauge invariance with abstract Regge theory (Phys. Letts. **B334**, 87). In recent papers, Claudio Corianò and White have presented an extensive study of the resulting kernel (Phys. Rev. Lett. **74**, 4980 and hep/ph 9503294, to be published in *Nucl. Phys.* B) . They detail the variety of Ward-identity constraints and infrared cancellations that characterize its infrared behaviour. They give an analytic form for the full non-forward kernel. For the forward kernel, which controls parton evolution at small-x , they give an impact parameter representation, derive the eigenvalue spectrum, and demonstrate a holomorphic factorization property related to conformal invariance. The results show that, at next-to-leading-order, the transverse momentum infrared region may produce a strong reduction of the BFKL small-x behavior.

In a new preprint (ANL-HEP-PR-95-12) Rajesh Parwani, Corianò, and White have further analyzed the non-leading kernel at nonzero momentum transfer. They have defined a complex extension and developed suitable regularizations of the corresponding diagrams, thereby providing a simplified expression for the full kernel. This investigation is expected to be essential in order to understand better the property of holomorphic factorization of the spectrum.

(A. White and C. Corianò)

II.A.5 Gauge Theory High-Energy Behavior from j-plane Unitarity

In a recent preprint (ANL-HEP-PR-95-19) Claudio Corianò and Alan White have shown that in a non-Abelian gauge theory the t-channel multiparticle unitarity equations continued in the complex j-plane can be systematically expanded around $j = 1$. The combination of Ward-identity constraints with unitarity is sufficient to produce directly many results obtained by Regge-limit leading-log and next-to-leading log momentum space calculations. The $\mathcal{O}(g^2)$ BFKL kernel is completely determined, as is the conformally invariant contribution to the $\mathcal{O}(g^4)$ kernel. This new formalism should establish the t-channel unitarity derivation of higher-order Regge behavior on a fundamental basis, directly comparable with s-channel unitarity calculations.

(A. White and C. Corianò)

II.A.6 Lattice Measurement of Matrix Elements for Decays of Heavy Quarkonium

Geoffrey Bodwin, Donald Sinclair, and Seyong Kim are continuing work on a project to to determine, in a lattice measurement, the nonperturbative operator matrix elements that appear in the expressions for the decay rates of S-wave and P-wave charmonium and bottomonium systems. This

work is based on the formalism for quarkonium decays developed by Bodwin, Braaten, and Lepage. The numerical simulations are described in the Computational Physics section of this report.

A part of this effort has involved the computation of the one-loop perturbative relations between the lattice operator matrix elements and the continuum ($\overline{MS}$) operator matrix elements. One needs to relate the lattice matrix elements to the continuum matrix elements because the latter appear in the existing expressions for quarkonium decay rates. Furthermore, the continuum matrix elements are more physical in that, owing to the absence of spurious, power ultraviolet divergences, they scale with the heavy-quark velocity according to simple rules that follow from nonrelativistic dynamics.

These computations are rather difficult technically, both because of the complicated Feynman rules that arise from lattice nonrelativistic QCD, and because one must subtract infrared divergences, which cancel between the lattice and continuum expressions, in such a way as to render the integrations over the lattice expressions numerically tractable.

The computation of the relations between the matrix elements has now been completed for the order v^0 and v^2 S-wave operators and the order v^2 P-wave operators. These are the leading and first subleading orders for the S-wave case and the leading order for the P-wave case. The S-wave operators are color singlets; the P-wave operators are a color singlet and a color octet. In the case of the the P-wave operators, the perturbative corrections turn out to be small — on the order of a few percent. In the case of the S-wave operators, the correction to the order v^2 operator was expected to be large, because of mixing with the order v^0 operator. This has turned out to be the case. As a consequence of this large correction, the results depend strongly on the choice of scale for the coupling constant α_s. An effort to compute the optimum scale by the method of Lepage and Mackenzie is now underway.

(G. Bodwin)

II.A.7 Inclusive Prompt Photon Production in Photon-Photon Collisions

Lionel Gordon and John K. Storrow (Manchester U.) are working on a complete next-to-leading-order calculation of prompt-photon production in photon-photon collisions in order to see whether this cross section will be of any use in determining the gluon distribution of the real photon. All fragmentation and non-fragmentation contributions are included, and the preliminary results suggest that the cross section will be measurable at LEP2.

(L. Gordon)

II.A.8 Analysis of Recent Polarization Experiments

High-energy polarization experiments can reveal valuable information regarding nucleon structure. Recently, polarized deep-inelastic scattering experiments were performed at SLAC and CERN. Gordon Ramsey and Mehrdad Goshtasbpour (Center for Theoretical Physics, Tehran) have done a theoretical analysis of deep-inelastic proton, neutron and deuteron data to extract this information from the corresponding structure functions. The integrals of these structure functions give information regarding the flavor dependence of spin, while a study of the Bjorken-x dependence can reveal the kinematical dependence of nucleon spin effects.

In a recent Argonne preprint ANL-HEP-PR-94-90 (submitted to *Physical Review* D), Ramsey and Goshtasbpour report results of their investigation of the integrated structure functions. They found discrepancies between the results which different sets of data yield. The proton and deuteron data imply a much larger polarized strange sea than the neutron data. Most theoretical models favor a smaller polarized sea. These differences do not appear to have an obvious kinematical dependence and remain even when higher-order QCD corrections are included in the analysis.

World averages of proton data imply that the quarks carry about one-third of the proton's spin. Analyses of neutron data give a somewhat larger value, while the deuteron data imply a smaller value. The large uncertainties in these values are decreased somewhat when higher-order QCD corrections are considered, but the differences remain. These experiments have shed light on the overall contributions of the quarks to the proton spin, but differ considerably regarding the specific flavor dependence of the spin.

Ramsey and Goshtasbpour are presently studying the Bjorken-x dependence of the structure functions using different parametrizations for the unpolarized distributions. This study includes an analysis of the polarized structure functions at small x and their relation to recent HERA experiments, which measured the unpolarized distributions. This could shed light on the differences seen in the integrated structure functions mentioned above.

More extensive deep-inelastic scattering experiments have been approved at SLAC and polarized lepton pair production (Drell-Yan) pp experiments are planned at RHIC. Ramsey has outlined how these experiments can resolve the differences mentioned above in an article published in *Particle World.*

(G. Ramsey)

II.B COMPUTATIONAL PHYSICS

The computational physics effort is devoted to numerical simulations of lattice quantum field theories, primarily of lattice quantum chromodynamics (QCD). The lattice provides the needed ultraviolet regulation of the theory and allows numerical simulations which are the only reliable way of calculating non-perturbative results from QCD. This enables one to investigate the behavior of hadronic/nuclear matter at finite temperature and finite baryon number density, and, in particular, to study the transition to a quark-gluon plasma. These calculations have relevance to the physics of the early universe, to neutron stars, and to relativistic heavy ion collisions (RHIC). In addition, lattice QCD enables us to calculate basic properties of hadrons, such as their masses and decay rates.

For some time we have been involved in a project aimed at calculating the matrix elements which describe the decays of charmonium and bottomonium into light hadrons, in collaboration with G. T. Bodwin of the theory group. We had previously calculated the matrix elements describing the decays of S- and P-wave bottomonium at $6/g^2 = 6.0$. Recently we have extended this to calculations at $6/g^2 = 5.7$, which has allowed us to calculate the matrix elements describing the decays of S- and P-wave charmonium, as well as recalculating the bottomonium matrix elements, to study their scaling properties. We have completed these calculations on small lattices ($8^3 \times 32$) on our Silicon Graphics Indigo work station, and are extending these calculations to $16^3 \times 32$ lattices on the CRAY C-90 at NERSC, allowing a quantitative study of finite size effects. In addition, we have

calculated the perturbative coefficients which relate the lattice matrix elements to the continuum matrix elements and are determining the renormalization scales at which these coefficients should be calculated.

For some time we have been involved in a collaboration with J. B. Kogut (University of Illinois) and M. P. Lombardo (Jülich) which has been studying hadronic matter at non-zero baryon number density (nuclear matter). During this period, we have completed a study of quenched QCD at finite temperature and small baryon number density. What we have found is that for chemical potentials (for quark number density) less than half the pion mass, the transition from hadronic matter to a quark-gluon plasma is similar to that for zero chemical potential. For larger chemical potentials we see signs of the anomalous behavior observed in the quenched theory at zero temperature. Our attempts to study full QCD at small baryon number density and finite temperature using complex Langevin methods have been thwarted by evidence that the complex Langevin algorithm fails, even in the absence of fermions when the action is real. These studies have been performed on the CRAY C-90 at NERSC and the CRAY T3D at PSC.

We have recently started calculations of the masses of flavor singlet mesons, in particular the η' and the $\sigma(f_0)$, in collaboration with J. B. Kogut (University of Illinois) and J.-F.Lagaë (University of Kentucky). These are of interest since they have a contribution from mixing with multi-gluon states. Because of this, the η' is sensitive to topological excitations (instantons, monopoles, etc.). For this reason, we intend to extend these calculations to non-zero temperature, to monitor the rôle of topological excitations in the transition from hadronic matter to a quark-gluon plasma. These studies are also using the CRAY C-90 at NERSC.

S. Kim has been collaborating with S. Ohta (Riken) to extend our calculations of the hadron spectrum of quenched lattice QCD at $6/g^2 = 6.5$ to a $48^3 \times 64$ lattice (our simulations were on a $32^3 \times 64$ lattice) to study finite size effects and to admit smaller quark masses. For these simulations they are using the Fujitsu VPP-500 at Riken.

(D. K. Sinclair, S. Kim)

III ACCELERATOR RESEARCH & DEVELOPMENT PROGRAM

III.A High Resolution Profile Monitor Development

Working toward eventual installation of the experiment at SLAC in September, followed by tests in December, we have designed and begun construction of most of the collimator vacuum chambers and precision collimator alignment system. Most shop work and vacuum hardware is done. An overall plan for control, cabling, and integration with the SLAC control system has been developed.

During the reporting period we did a test run, with beam, at the SLAC Final Focus Test Beam (FFTB). We set up a prototype detector, camera and computer behind the E144 pair spectrometer in the FFTB beamline and measured backgrounds under a variety of conditions. The backgrounds seemed sufficiently low to permit detection of Čerenkov photons from the pairs produced in the γ conversion target. Along with the data taken at BATES/MIT, these measurements show that the signal/noise ratio with a Compton conversion source should be good.

In order to make precise measurements of linear collider beam spots, it is necessary to understand ground vibrations, which can be many times larger than the expected spot sizes. After the Streckeisen STS-2 seismometer was used for initial checkout tests, there were limited possibilities for accelerator relevant experiments at Argonne using a single device. Following a request from the USGS in Menlo Park, our unit was loaned to experimenters developing devices for a future Mars mission. After the completion of this experiment, the seismometer was sent to SLAC along with another device loaned by the USGS. Experiments are now underway, during a SLAC shutdown, which will measure the spectrum and correlations of ground noise using two points at varying separations. This noise will determine some of the ulitmate limits to the resolution of our measurement technique, and may determine the ultimate maximum energy which can be reached in linear colliders, since the required beamspot size must decrease like (beam energy)$^{-2}$, and this size is likely to be limited by seismic vibrations.

The design of a high power proton source needed to provide the large number of muons is among the issues that is critical to the possible construction of a $\mu - \mu$ collider. We have begun to look at options for a 10 GeV synchrotron, and have begun to consider a system with a 1 GeV injector and about 1.5 MV/turn of accelerating field. The final short bunch on target can be generated from many smaller bunches which would be extracted using a single turn and combined using beamlines of different lengths.

(J. Norem)

IV. PUBLICATIONS

A. Journal Publications, Conference Proceedings, Books

A Scheme for Radiative CP Violation
W.-Y. Kueng, D. Chang (ANL)
Phys. Rev. Lett. 74, 1928 (1995)

A Search for Excited Fermions in Electron-Proton Collisions at HERA
M. Derrick, D. Krakauer, S. Magill, B. Musgrave, J. Repond, J. Schlereth, R. Stanek, R. Talaga, J. Thron (ANL) and the ZEUS Collaboration
Z. Phys. C65, 627 (1995)

Charge Asymmetry in W-Boson Decays Produced in $p\bar{p}$ Collisions at $\sqrt{s} = 1.8$ TeV
R. Blair, K. Byrum, T. Fuess, S. Kuhlmann, L. Nodulman, J. Proudfoot, R. Wagner, A. Wicklund (ANL) and the CDF Collaboration
Phys. Rev. D. V74, 850 (1995)

Dijet Cross Sections in Photoproduction at HERA
M. Derrick, D. Krakauer, S. Magill, D. Mikunas, B. Musgrave, J. Repond, R. Stanek, R. Talaga, H. Zhang (ANL) and the ZEUS Collaboration
Phys. Lett. B348, 665 (1995)

Direct Measurement of the W Boson Width
R. Blair, K. Byrum, T. Fuess, S. Kuhlmann, L. Nodulman, J. Proudfoot, R. Wagner, A. Wicklund (ANL) and the CDF Collaboration
Phys. Rev. Lett. V 74, 341 (1995)

Electroweak Physics from the Tevatron
L. Nodulman
Proceedings of Tennessee Int'l. Symposium on Radiative Corrections, edited by B.L.F. Ward, World Sci, 73 (1995)

Extraction of the Gluon Density of the Proton at Small x
Observation of Hard Scattering in Photoproduction Events with a Large Rapidity Gap at HERA
M. Derrick, D. Krakauer, S. Magill, B. Musgrave, J. Repond, J. Schlereth, R. Stanek, R. Talaga, J. Thron (ANL) and the ZEUS Collaboration
Phys. Lett. B345, 576 (1995)

Higher-Order Lipatov Kernels and the QCD Pomeron
A. White (ANL)
Proceedings of the Workshop on Quantum Infra-Red Physics, edited by H. Fried and B. Muller, what is page number? (1995)

Inclusive Transverse Momentum Distributions of Charged Particles in Diffractive and Non-Diffractive Photoproduction at HERA
M. Derrick, D. Krakauer, S. Magill, D. Mikunas, B. Musgrave, J. Repond, R. Stanek, R. Talaga, H. Zhang (ANL) and the ZEUS Collaboration
Zeitschrift fur Physik C67, 227 (1995)

Inclusive Jet Differential Cross-Sections in Photoproduction at HERA
M. Derrick, D. Krakauer, S. Magill, B. Musgrave, J. Repond, J. Schlereth, R. Stanek, R. Talaga, J. Thron (ANL) and the ZEUS Collaboration
Phys. Lett. B342, 417 (1995)

Jet Production in High Q^2 Deep-Inelastic ep Scattering at HERA

M. Derrick, D. Krakauer, S. Magill, D. Mikunas, B. Musgrave, J. Repond, R. Stanek, R. Talaga, H. Zhang (ANL) and the ZEUS Collaboration
Zeitschrift fur Physik C67, 81 (1995)

Kinematic Evidence for Top Quark Pair Production in W + Multijet Events in $p\bar{p}$ Collisions at $\sqrt{s} = 1.8$ TeV
R. Blair, K. Byrum, T. Fuess, S. Kuhlmann, L. Nodulman, J. Proudfoot, R. Wagner, A. Wicklund (ANL) and the CDF Collaboration
Phys. Rev. D. V51, 4623 (1995)

Limits on Z-Photon Couplings from $p-\bar{p}$ Interactions at $\sqrt{s} = 1.8$ TeV
R. Blair, K. Byrum, D. Crane, T. Fuess, S. Kuhlmann, L. Nodulman, J. Proudfoot, R. Wagner, A. Wicklund (ANL) and the CDF Collaboration
Phys. Rev. Lett., V74, 1941 (1995)

Measurement of Multiplicity and Momentum Spectra in the Current Fragmentation Region of the Breit Frame at HERA
M. Derrick, D. Krakauer, S. Magill, D. Mikunas, B. Musgrave, J. Repond, R. Stanek, R. Talaga, H. Zhang (ANL) and the ZEUS Collaboration
Zeitschrift fur Physik C67, 93 (1995)

Measurement of Single Spin Asymmetry for Direct Photon Production in pp Collisions at 200 GeV/C
D. Grosnick, D. Hill, D. Lopiano, Y. Ohashi, T. Shima, H. Spinka, D. Underwood, A. Yokosawa
Phys. Lett. B 345, 569 (1995)

Measurement of the Cross Section for the Reaction $\gamma p \rightarrow Jx p$ with the ZEUS Detector at HERA
M. Derrick, D. Krakauer, S. Magill, D. Mikunas, B. Musgrave, J. Repond, R. Stanek, R. Talaga, H. Zhang (ANL) and the ZEUS Collaboration
Phys. Lett. B350, 120 (1995)

Measurement of the Proton Structure Function F_2 from the 1993 HERA Data
M. Derrick, D. Krakauer, S. Magill, B. Musgrave, J. Repond, J. Schlereth, R. Stanek, R. Talaga, J. Thron (ANL) and the ZEUS Collaboration
Z. Phys. C65, 379 (1995)

Measurement of W-Photon Couplings in $p-\bar{p}$ Collisions at $\sqrt{s} = 1.8$ TeV
R. Blair, K. Byrum, T. Fuess, S. Kuhlmann, L. Nodulman, J. Proudfoot, R. Wagner, A. Wicklund (ANL) and the CDF Collaboration
Phys. Rev. Lett., V74, 1936 (1995)

New Strong Interactions above the Electroweak Scale
A. White (ANL)
Proceedings of the VIII International Symposium on Very High Energy Cosmic Ray Interactions, edited by Y. Fujimoto, *et. al.*, 468 (1994)

Observation of Hard Scattering in Photoproduction Events with a Large Rapidity Gap at HERA
M. Derrick, D. Krakauer, S. Magill, B. Musgrave, J. Repond, J. Schlereth, R. Stanek, R. Talaga, J. Thron (ANL) and the ZEUS Collaboration
Phys. Lett. B346, 399 (1995)

Observation of Rapidity Gaps in $\bar{p}p$ Collisions at 1.8 TeV
R. Blair, K. Byrum, T. Fuess, S. Kuhlmann, L. Nodulman, J. Proudfoot, R. Wagner, A. Wicklund (ANL) and the CDF Collaboration
Phys. Rev. Lett. V 74, 855 (1995)

Observation of Top Quark Production in $\bar{p}p$ Collisions with the Collider Detector at Fermilab
R. Blair, K. Byrum, T. Fuess, S. Kuhlmann, L. Nodulman, J. Proudfoot, R. Wagner, A. Wicklund (ANL) and the CDF Collaboration
Phys. Rev. Lett. V 74, 2626 (1995)

Scale-Invariant Lipatov Kernels from t-Channel Unitarity
C. Coriano and A White (ANL)
Proceedings of the XXIV Int'l. Symposium on Multiparticle Dynamics, edited by A. Giovannini, S. Lupia, and R. Ugoccioni, 309 (1995)

Search for Charged Bosons Heavier than the W Boson in $= 1.8$ TeV $p\bar{p}$ Collisions at $\sqrt{s} = 1800$ GeV
R. Blair, K. Byrum, T. Fuess, S. Kuhlmann, L. Nodulman, J. Proudfoot, R. Wagner, A. Wicklund (ANL) and the CDF Collaboration
Phys. Rev. Lett. V74, 2900 (1995)

Search for New Gauge Bosons Decaying into Dielectrons in $\bar{p}p$ collisions at $\sqrt{s} = 1.8$ TeV
R. Blair, K. Byrum, T. Fuess, S. Kuhlmann, L. Nodulman, J. Proudfoot, R. Wagner, A. Wicklund (ANL) and the CDF Collaboration
Phys. Rev. D. V51, R949 (1995)

Search for New Particles Decaying to Dijets in $\bar{p}p$ collisions at $\sqrt{s} = 1.8$ TeV
R. Blair, K. Byrum, D. Crane, T. Fuess, S. Kuhlmann, L. Nodulman, J. Proudfoot, R. Wagner, A. Wicklund (ANL) and the CDF Collaboration
Phys. Rev. Lett. V74, 3538 (1995)

Study of $D^*(2010)^{\pm}$ Production in *ep* Collisions at HERA
M. Derrick, D. Krakauer, S. Magill, D. Mikunas, B. Musgrave, J. Repond, J. Schlereth, R. Stanek, R. Talaga, H. Zhang (ANL) and the ZEUS Collaboration
Phys. Lett. B349, 225 (1995)

The Atmospheric Neutrino Anomaly in Soudan 2
M. Goodman, I. Ambats, D. Ayres, L. Balka, W. Barrett, J. Dawson, T. Fields, N. Hill, J. Hofteizer, D. Jankowski, F. Lopez, E. May, L. Price, J. Schlereth, J. Thron, J. Uretsky (ANL) and the Soudan 2 Collaboration
Nucl. Phys. B Proceedings Supplements 38, 337(1995)

The High Energy Behavior of the Forward Scattering Parameters -- σ_{tot}, ρ, and B
A. White (ANL), *et. al.*
Proceedings of the XXIV Int'l. Symposium on Multiparticle Dynamics, edited by A. Giovannini, S. Lupia, and R. Ugoccioni, 478 (1995)

The Phases and Triviality of Scalar Quantum Electrodynamics
S. Kim (ANL), *et. al.*,
Phys. Rev. D51, 5216 (1995)

The ZEUS Calorimeter First Level Trigger
J. Dawson, D. Krakauer, J. Schlereth, R. Talaga (ANL), *et. al.*,
Nucl. Phys. and Meth. A360, 322 (1995)

B. Papers Submitted for Publication and ANL Reports

Evidence for Hard Chiral Logarithms in Quenched Lattice QCD
S. Kim and D. Sinclair (ANL)
ANL-HEP-PR-95-5
Submitted to Phys. Rev. D

The U(1) Gross-Neveu Model at Non-Zero Chemical Potential
S. Kim
ANL-HEP-PR-95-7
Submitted to Nucl. Phys. B

C. Papers or Abstracts Contributed to Conferences

Drell-Yan Pairs, W± and Z Event Rates and Background at RHIC
A. Yokosawa
ANL-HEP-CP-95-10
Submitted to Proceedings of 11th Int'l. Symposium in HE Spin Physics and 8th Symposium on Polarization Phenomena in Nucl. Phys., Bloomington, IN

CDF Results on $Z\gamma$ Production
R. Wagner
ANL-HEP-CP-95-20
Submitted to Proceedings of Int'l. Symposium on Vector Self-Interactions, LA, CA

WW and WZ Production at the Tevatron
T. Fuess
ANL-HEP-CP-95-25
Submitted to Proceedings of Int'l. Symposium on Vector Self-Interactions, LA, CA

Conformally Symmetric Contributions to BFKL Evolution at Next to Leading Order
C. Coriano and A. White
ANL-HEP-CP-95-27
Submitted to Proceedings of XXXth Recontres de Moriond, Les Arcs, France

Prospects for Spin Physics at RHIC
R. Robinett
ANL-HEP-CP-95-28
Submitted to Proceedings of Int'l. Symposium on Particle Theory

The Argonne Wakefield Accelerator High Current Photocathode Gun and Drive Linac
P. Schoessow, E. Chojnacki, W. Gai, C. Ho, R. Simpson
ANL-HEP-CP-95-34
Submitted to Proceedings of the 1995 PAC Conference, Dallas, TX

Witness Gun for the Argonne Wakefield Accelerator
J. Power, J. Simpson, E. Chojnacki, R. Konecny
ANL-HEP-CP-95-35
Submitted to Proceedings of the 1995 PAC Conference, Dallas, TX

D. Technical Notes

Module Strap Tests and How They Effect the 25 cm Stack Construction
N. Hill
ANL-HEP-TR-95-04

Efficiency of Modified UA1 Jet Reconstruction Algorithm in PP, PA and AA Collisions at STAR
K. Shestermanov (ANL visitor) and B. Christie (BNL)
ANL-HEP-TR-95-11, STAR Note #196

High Energy Physics Division Semi-Annual Report (July 1-December 31, 1994)
R. Wagner, P. Schoessow, R. Talaga
ANL-HEP-TR-95-26

Trip Report for Trip to Steel Warehouse Inc. Southbend Indiana
N. Hill
ANL-HEP-TR-95-32

Technical Specification for Plate Fabrication for the Atlas Tile Hadron Calorimeter
N. Hill
ANL-HEP-TR-95-39

NuMI-L-49 Standard Event Rate Assumptions for January 1995 Long Baseline Proposal Document
M. Goodman

NuMI-L-54 Report of LBNE Detector R&D Committee
D. Ayres (ANL) *et. al.*

NuMI-L-57 Report of the Long Baseline Experiment Naming Committee
M. Goodman (ANL) M. Michael

NuMI-L-59 Unofficial notes on the Long Baseline Collaboration Meeting at Fermilab January 9-13, 1995
D. Ayres

NuMI-L-63 MINOS proposal (February 9, 1995)
D. Ayres, *et. al.*

NuMI-L-64 Near/Far Differences (and Similarities) in the NuMI Beam
D. Crane, M. Goodman

NuMI-L-71 Summary of MINOS Proposal, A Beamline Oscillation Experiment at Fermilab
D. Ayres

NuMI-L-77 Minutes of the MINOS Collaboration Meeting at Fermilab, April 8-9- 1995
D. Ayres

NuMI-L-79 Addendum to P-875: A Long-baseline Neutrino Oscillation Experiment at Fermilab (April 21, 1995)
D. Ayres (ANL), *et. al.*

NuMI-L-80 Response to PAC Question No. 2 relating to the NuMI Beam Line
D. Crane (ANL), *et. al.*

NuMI-L-84 Minutes of a MINOS Electronics Discussion at Oxford on 22-Mar-95
J. Thron

NuMI-L-86 Minutes of the MINOS Executive Committee Meeting of 9 April 1995
M. Goodman

NuMI-B-87 Trip Reports of the NuMI Beam Group to CERN, March 1995
D. Crane (ANL) *et. al.*

NuMI-L-89 Minutes of the MINOS Collaboration Meeting at Fermilab May 20-21, 1995
D. Ayres

NuMI-L-96 MINOS Answers to HEPAP Subpanel Questions
D. Ayres (ANL) *et. al.*

PDK-609 Soudan 2 Experiment Quarterly Status Report October - December 1994

D. Ayres

PDK-613 Decisions of the Oxford Collaboration Meeting March 21-24, 1995
D. Ayres

PDK-614 Soudan 2 Experiment Quarterly Status Report January - March 1995
D. Ayres

PDK-615 Effects of Misidentification of Events
H. Gallagher, R. Seidlein

V COLLOQUIA AND CONFERENCE TALKS

R. Blair

"Photon Plus Charm and Diphoton Production at $\sqrt{s}$=1.8 TeV"
10^{th} Topical Workshop on Proton-Antiproton Collider Physics Fermilab (May, 1995)

G. Bodwin

"Production and Decay of Heavy Quarkonia: New Factorization Theorems"
Physics Division, Argonne National Laboratory (January, 1995)

T. Fields

"Searching for Neutrino Oscillations at Soudan"
Physics Department, University of Hawaii, Honolulu (January, 1995)

J. Repond

"A Tau-Charm Factory at Argonne"
Town Meeting on Nuclear Physics, Physics Division, Argonne (January, 1995)
Physics Department, McGill University, Montreal, Canada (April, 1995)

"Measurement of the Gluon Density at HERA"
Physics Department, University of Maryland, College Park (February, 1995)
Luncheon Seminar, High Energy Physics Division, Argonne (February, 1995)

R. Talaga

"Recent Results from HERA"
Physics Department, University of Chicago (May, 1995)
Luncheon Seminar, High Energy Physics Division, Argonne (June, 1995)

A. White

"The t-channel Unitarity Construction of Small-x Kernels"
Lecture Series at the $XXXV^{th}$ (Jubilee) Cracow School of Theoretical Physics, Zakopane, Poland. (June, 1995)

"Higher-order BFKL Corrections from t-channel Unitarity"
Theory Seminar, DESY Laboratory, Hamburg, Germany (June,1995)
VI^{th} International Conf. on Elastic Scattering and Diffraction, Blois, France (June, 1995)

"Is the Higgs Sector Just Π_6 in the Sky?"
Luncheon Seminar, High Energy Physics Division, Argonne (February, 1995)

A. Yokosawa

"RHIC Spin Physics"
Physics Department, Wayne State University, Detroit (April, 1995)

"Spin Physics with STAR"
RHIC Spin Collaboration Meeting, Massachusetts Institute of Technology, Cambridge, Massachusetts (May, 1995)

VI HIGH ENERGY PHYSICS COMMUNITY ACTIVITIES

E. Berger
Member, Committee on Meetings, American Physical Society, 1991-present

Member, RHIC Spin Review Committee, Brookhaven National Laboratory, June, 1995

Member, U.S. Contact person, Scientific Program Committee, XXX Rencontre de Moriond, "QCD and High Energy Hadronic Interactions", Meribel, France, March, 1995

Member, Local Organizing Committee, 10^{th} Topical Workshop on Proton-Antiproton Collider Physics, Fermilab, May 9-13, 1995

Member, American Physical Society Task Force on Forums, 1995

Chairman, Argonne Laboratory Director's Review Committee, Individual Investigator Laboratory Directed Research and Development Program, 1994-1995

Member, Local Organizing Committee, Tau-Charm Factory Workshop, Argonne National Laboratory, June, 1995

Member, High Energy and Nuclear Physics Advisory Committee, Brookhaven National Laboratory, 1995-1998

Member, International Advisory Committee, Snowmass Summer Study, Division of Particles and Fields of the American Physical Society, Snowmass, CO, June-July, 1996

Member, Steering Committee, 11^{th} Topical Workshop on Hadron Collider Physics, Padova, Italy 1996

Organizing Committee, Sixth Conference on the Intersections between Particle and Nuclear Physics, May, 1997

T. Fields
Member, Universities Research Association Visiting Committee for Fermilab

S. Kuhlmann
Member, Fermilab Users Facilities Committee

Member, Organizing Committee, CTEQ Workshop on Top Production, Fermilab, April 5-7, 1995

J. Thron
Member, MINOS Technical Board

A. Yokosawa
Member, International Advisory Committee for the Adriatico Conference on Trends in Collider Spin Physics, Trieste, Italy (February, 1995)

C. Zachos
Member, Editorial Board of the Journal of Physics A: Mathematical and General Physics

VII HIGH ENERGY PHYSICS DIVISION RESEARCH PERSONNEL

Administration

L. Price
D. Hill

Accelerator Physicists

W. Gai
J. Norem
P. Schoessow
J. Simpson

Experimental Physicists

D. Ayres
R. Blair
K. Byrum
D. Crane
M. Derrick
T. Fields
T. Fuess
M. Goodman
D. Grosnick
D. Krakauer
S. Kuhlmann
D. Lopiano
S. Magill
E. May
B. Musgrave
L. Nodulman
J. Proudfoot
J. Repond
R. Seidlein
H. Spinka
R. Stanek
R. Talaga
J. Thron
D. Underwood
R. Wagner
A. B. Wicklund
A. Yokosawa

Theoretical Physicists

E. Berger
G. Bodwin
H. Contopanagos
C. Corianò
L. Gordon
S.-Y. Kim
D. Sinclair
A. White
C. Zachos

Engineers, Computer Scientists, and Applied Scientists

J. Dawson
V. Guarino
W. Haberichter
N. Hill
J. Nasiatka
J. Schlereth
X. Yang

Technical Support Staff

I. Ambats
L. Balka
H. Blair
G. Cox
D. Jankowski
T. Kasprzyk
L. Kocenko
D. Konecny
R. Rezmer

Laboratory Graduate Participants

C. Allgower
N. Barov
H. Gallagher
M. Hohlmann
H. Huang
D. Mikunas
J. Power
H. Zhang

Visiting Physicists

M. Conde(AWA)
T. Curtright(Theory)
A. Davidenko(STAR)
P. Freund(Theory)
G. Gerster(Theory)
T. Huang(Theory)
R. Meng(Theory)
R. Parwani(Theory)
G. Ramsey(Theory)
R. Robinett(Theory)
L. Rozansky(Theory)
K. Shestermanov(STAR)
J. Uretsky(Theory/Soudan)
C.-P. Yuan(Theory)